Quaternion-Based Hybrid Control for Robust Global Attitude Tracking*

Christopher G. Mayhew[†], *Member, IEEE,* Ricardo G. Sanfelice[‡], *Member, IEEE,* Andrew R. Teel[þ] *Fellow, IEEE*

***Abstract*—It is well known that controlling the attitude of a rigid body is subject to topological constraints. We illustrate, with examples, the problems that arise when using continuous and (memoryless) discontinuous quaternion-based state-feedback control laws for global attitude stabilization. We propose a quaternion-based hybrid feedback scheme that solves the global attitude tracking problem in three scenarios: full state measurements, only measurements of attitude, and measurements of attitude with angular velocity measurements corrupted by a constant bias. In each case, the hybrid feedback is *dynamic* and incorporates hysteresis-based switching using a single binary logic variable for each quaternion error state. When only attitude measurements are available or the angular rate is corrupted by a constant bias, the proposed controller is observer-based and incorporates an additional quaternion filter and bias observer. The hysteresis mechanism enables the proposed scheme to simultaneously avoid the "unwinding phenomenon" and sensitivity to arbitrarily small measurement noise that is present in discontinuous feedbacks. These properties are shown using a general framework for hybrid systems and the results are demonstrated by simulation.**

I. Introduction

A. Motivation and Background

Achieving robust global asymptotic stability of the attitude of a rigid body is rife with topological difficulty stemming from the very structure of the rigid body state space: the special orthogonal group of order three, denoted $SO(3)$. In particular, $SO(3)$ is not a vector space–it is a boundaryless compact manifold, which, as a result of degree theory, implies that it does not have the topological property of contractibility [1, Ex. 2.4.6]. Furthermore, the basin of attraction of an asymptotically stable equilibrium point of a differential equation with a locally Lipschitz right-hand side is necessarily contractible [2] and in fact, homeomorphic to some Euclidean space [3, Theorem V.3.4]. Since $SO(3)$ is not diffeomorphic to any Euclidean space (it is not contractible), it is *impossible* for any continuous state-feedback control law to render some equilibrium point of $SO(3)$ (or its tangent bundle) globally asymptotically stable [4]. In fact, [5] points out that any smooth vector field on $SO(3)$ with an attracting equilibrium point must have at least one other equilibrium point that is unstable.

Continuous state-feedback control laws on $SO(3)$ are at most *almost* globally stabilizing, where the basin of attraction necessarily excludes a nowhere dense set of zero Lebesgue measure. For instance, the controllers proposed in [6]–[8] vanish at attitudes that are 180° from the desired attitude about the principal axes of the rigid body when the angular velocity is zero, creating three saddle equilibria (or, in the case of [9], an unstable connected 2-D manifold) and one almost globally asymptotically stable equilibrium. The *reduced* attitude stabilization problem has similar issues as its dynamics evolve on $\mathcal{S}^2$, the unit 2-sphere, which is also compact and boundaryless. Indeed, the smooth controller proposed in [8] is *almost* globally stabilizing. A similar nonsmooth controller proposed in [10] makes for a simple description of the basin of attraction, but is undefined at some attitudes and results in an unbounded feedback. These topological issues arise in other applications involving rotational degrees of freedom, like pendulum systems [11], robotic manipulators [12], and gimbal-pointing mechanisms (e.g. a pan-tilt camera) [13], among others (see [4, Table 1] for several examples).

Rigid-body attitude is often parametrized to exploit redundancies in the rotation-matrix description of $SO(3)$; however, certain parametrizations face further topological difficulties. As pointed out in [14], no three-parameter parametrization of $SO(3)$ is globally nonsingular (i.e., the map from representation coordinates to $SO(3)$ is not everywhere a local diffeomorphism). This creates an inherent obstacle in achieving global asymptotic stability using control methods based on Euler angles (e.g. pitch, roll, yaw), (modified) Rodrigues parameters, and exponential coordinates, among others.

Pursuing a globally nonsingular parametrization, many authors (as well as the authors of this paper) employ unit quaternions, which evolve on the three-dimensional unit sphere, denoted $\mathcal{S}^3$. Because there are exactly two antipodal unit quaternions corresponding to the same attitude in $SO(3)$, the attitude-control objective in $\mathcal{S}^3$ is to stabilize the *disconnected* set of quaternions representing the same physical attitude. When this double-covering is neglected (e.g., in [15]–[20]), the resulting controller can induce *unwinding*, causing the rigid body to unnecessarily make a full rotation [4], [15]–[17].

The problem of robustly and globally asymptotically stabilizing a *disconnected* set of points has its own topological issues. In fact, [21] shows that it is impossible to accomplish this task with a (memoryless) discontinuous state-feedback in a way that is robust to measurement noise. We show here that when discontinuous control (e.g. [22]–[25]) is used in

[†]christopher.mayhew@us.bosch.com, Robert Bosch Research and Technology Center, 4009 Miranda Ave., Palo Alto, CA 94304

[‡]sricardo@u.arizona.edu, Department of Aerospace and Mechanical Engineering, University of Arizona, Tucson, AZ 85721.

[þ]teel@ece.ucsb.edu, Center for Control Engineering and Computation, Electrical and Computer Engineering Department, University of California, Santa Barbara, CA 93106-9560.

*Research partially supported by the National Science Foundation under Grant no. ECCS-0925637 and Grant no. CNS-0720842, and by the Air Force Office of Scientific Research under Grant no. FA9550-09-1-0203.

an attempt to break the topological constraints for global stabilization on $SO(3)$, the introduction of arbitrarily small measurement noise can destroy any global attractivity property. This is a common problem for topologically constrained control problems and has been investigated in [21], [26], for example. A classic example where dynamics constrain the state to move along circles in $\mathbb{R}^2$ is provided in [27] (discussed again in [28]), which suffers similar issues.

B. Contributions

In this paper, we propose a quaternion-based hybrid feedback that breaks the topological obstructions to global asymptotic stability on $SO(3)$ and concurrently defeats problems induced by measurement noise. The proposed scheme is applicable to any quaternion-based attitude control problem and we apply it to three attitude tracking scenarios: full state measurements, only attitude measurements, and full state measurements where the angular velocity measurement is corrupted by an unknown constant bias. In each case, the hybrid controller maintains a single binary logic variable per quaternion state to implement hysteresis-based switching of control laws. When the latter two cases are addressed, the hybrid controller incorporates an additional quaternion filter and bias estimate. The price to pay for robust global asymptotic stabilization with the proposed scheme is a small region in the state space where the hybrid control law pulls the rigid body in the direction of a longer rotation, though the amount is controlled by a user-defined hysteresis width that is usually selected to be commensurate with the anticipated noise magnitude.

This paper is organized as follows. Section II gives a brief review of attitude representations, unit-quaternion algebra, and rigid body kinematics and dynamics. Section III discusses how topological constraints arise when using quaternion-based feedback. Section IV serves to derive the open-loop error system and pose the tracking objective as a compact set stabilization problem for an autonomous system. Section V proposes hybrid control schemes for robust tracking in several output feedback scenarios, and finally, Section VI shows a simulation study where the proposed hybrid controller is compared to its discontinuous and unwinding-inducing analogs.

II. Rigid Body Attitude: Representation, Quaternion Algebra and Dynamics

The attitude of a rigid body is described by a 3×3 rotation matrix. The set of 3×3 rotation matrices with unitary determinant is the *special orthogonal group* of order three,

$$SO(3) = \{R \in \mathbb{R}^{3\times 3} : R^\top R = RR^\top = I,\ \det R = 1\}.$$

For any $x \in \mathbb{R}^3$, we let

$$S(x) = \begin{bmatrix} 0 & -x_3 & x_2 \\ x_3 & 0 & -x_1 \\ -x_2 & x_1 & 0 \end{bmatrix},$$

so that for two vectors $x, y \in \mathbb{R}^3$, $x \times y = S(x)y$, where $\times$ denotes the vector cross product.

In this paper, the attitude of a rigid body $R \in SO(3)$ will denote a rotation of vector coordinates expressed in the body frame to vector coordinates expressed in an inertial frame. Let $\omega \in \mathbb{R}^3$ denote the angular velocity given in the body frame, let $\mathcal{J} = \mathcal{J}^\top > 0$ denote the inertia matrix of the rigid body, and let τ denote a vector of external torques. Then, the rigid body satisfies the kinematic and dynamic equations

$$\begin{aligned} \dot{R} &= RS(\omega) \\ \mathcal{J}\dot{\omega} &= S(\mathcal{J}\omega)\omega + \tau \end{aligned} \qquad (R,\omega) \in SO(3) \times \mathbb{R}^3. \qquad (1)$$

Let the n-dimensional unit sphere embedded in $\mathbb{R}^{n+1}$ be denoted as $\mathcal{S}^n = \{x \in \mathbb{R}^{n+1} : x^\top x = 1\}$. Then an element of $SO(3)$ can be parametrized by a unit quaternion

$$q = \begin{bmatrix} \eta & \epsilon^\top \end{bmatrix}^\top \in \mathcal{S}^3, \qquad (2)$$

through the Rodrigues formula $\mathcal{R} : \mathcal{S}^3 \to SO(3)$ defined as

$$\mathcal{R}(q) = I + 2\eta S(\epsilon) + 2S(\epsilon)^2. \qquad (3)$$

We note that mapping $\mathcal{R} : \mathcal{S}^3 \to SO(3)$ is everywhere a local diffeomorphism, but globally two-to-one and satisfies $\mathcal{R}(q) = \mathcal{R}(-q)$. For convenience, we may refer to a unit quaternion as a pair $q = (\eta, \epsilon)$ rather than as a vector and we note that $\eta \in \mathbb{R}$ and $\epsilon \in \mathbb{R}^3$ are commonly referred to as the "scalar" and "vector" components of $q \in \mathcal{S}^3$.

Multiplication between two quaternions, $q_i = (\eta_i, \epsilon_i)$, $i \in \{1, 2\}$, is defined as

$$q_1 \otimes q_2 = \begin{bmatrix} \eta_1\eta_2 - \epsilon_1^\top\epsilon_2 \\ \eta_1\epsilon_2 + \eta_2\epsilon_1 + S(\epsilon_1)\epsilon_2 \end{bmatrix}.$$

With the identity element $\mathbf{1} = (1, 0)$, each $q = (\eta, \epsilon) \in \mathcal{S}^3$ has an inverse, $q^{-1} = (\eta, -\epsilon)$, so that $q^{-1} \otimes q = q \otimes q^{-1} = \mathbf{1}$. Quaternion multiplication is analogous to multiplication between elements of $SO(3)$, in that $\mathcal{R}(q_1)\mathcal{R}(q_2) = \mathcal{R}(q_1 \otimes q_2)$.

When representing R with a unit quaternion q, we must "lift" the kinematic equation (1) onto $\mathcal{S}^3$. Suppose that $\omega : \mathbb{R}_{\geq 0} \to \mathbb{R}^3$ is measurable, $R : \mathbb{R}_{\geq 0} \to SO(3)$ is absolutely continuous and satisfies (1), and let $\nu : \mathbb{R}^3 \to \mathbb{R}^4$ be defined as the mapping

$$\nu(x) = \begin{bmatrix} 0 & x^\top \end{bmatrix}^\top.$$

Then, if for every $t \in \mathbb{R}_{\geq 0}$ an absolutely continuous mapping $q : \mathbb{R}_{\geq 0} \to \mathcal{S}^3$ satisfies $\mathcal{R}(q(t)) = R(t)$, then $\dot{q}$ satisfies

$$\dot{q} = \begin{bmatrix} \dot{\eta} \\ \dot{\epsilon} \end{bmatrix} = \frac{1}{2} q \otimes \nu(\omega) = \frac{1}{2} \begin{bmatrix} -\epsilon^\top \\ \eta I + S(\epsilon) \end{bmatrix} \omega. \qquad (4)$$

From the path lifting property, we recall that such a trajectory q is unique up to its initial condition (of which there are two that satisfy $\mathcal{R}(q(0)) = R(0)$) [29]. We refer the reader to [30] for a more complete description of attitude representation and rigid body dynamics, and to [31] for a wealth of information about unit quaternions.

III. Quaternion-Based Attitude Control

To elucidate the topological issues discussed in Section I, we consider the problem of designing a globally asymptotically stabilizing control law for the identity element of $SO(3)$ with a unit quaternion representation using ω as the control variable.

Preprint submitted to IEEE Transactions on Automatic Control. Received: January 18, 2011 20:37:59 PST

One might see (1) as a singular perturbation of the kinematics or as the start of a backstepping procedure (see e.g. [25], [32]). The following discussion is of independent interest when quaternion filters are used (as in [20], [23], as well as in this paper) and also applies to designing a torque feedback, which we consider in the sequel.

Our goal is to design a velocity feedback to stabilize $q = (\eta, \epsilon) = \pm\mathbf{1} = (\pm 1, 0)$ for the system (4). Suppose one overlooks the double-cover property indicated above and uses the Lyapunov function (see, for example, [15]–[20], [33])

$$\widehat{V}_1(q) = 2(1-\eta) = (1-\eta)^2 + \epsilon^\top \epsilon. \tag{5}$$

It is obvious that $\widehat{V}_1(q) = 0$ if and only if $q = \mathbf{1}$ and that $\widehat{V}_1(\mathcal{S}^3 \setminus \{\mathbf{1}\}) > 0$. Note further that $\widehat{V}_1$ achieves its maximum over $\mathcal{S}^3$ at $q = -\mathbf{1}$.

With the feedback $\omega = \phi_1(q) := -\epsilon$, we have

$$\left\langle \nabla \widehat{V}_1(q), \tfrac{1}{2} q \otimes \nu(\phi_1(q)) \right\rangle = -\epsilon^\top \epsilon,$$

which is negative for all $q \in \mathcal{S}^3 \setminus \{\pm\mathbf{1}\}$. This particular choice of feedback law generates two closed-loop equilibrium points: $q = -\mathbf{1}$ (unstable) and $q = \mathbf{1}$ (stable). Since both $+\mathbf{1}$ and $-\mathbf{1}$ represent the same point in $SO(3)$, the desired attitude can be stable or unstable, depending on the controller's knowledge of the quaternion representation! Note that using $\widehat{V}_1(-q)$ and the control law $\phi_1(-q) = \epsilon$ has much the same effect on stability by stabilizing $-\mathbf{1}$ and destabilizing $+\mathbf{1}$. This point is illustrated in Fig. 1 and discussed further in [4], [15], [16]. In particular, [4] discusses how this control law leads to *unwinding*.

To avoid unwinding, one can employ the Lyapunov function

$$\widehat{V}_2(q) = 1 - \eta^2 = \epsilon^\top \epsilon = \tfrac{1}{4} \operatorname{trace}(I - \mathcal{R}(q)).$$

Clearly, $\widehat{V}_2$ satisfies $\widehat{V}_2(q) = 0$ if and only if $q = \pm\mathbf{1}$ and $\widehat{V}_2(\mathcal{S}^3 \setminus \{\pm\mathbf{1}\}) > 0$. Note that $\widehat{V}_2(q) = \widehat{V}_2(-q)$ and that $\widehat{V}_2$ achieves its maximum value on

$$\mathcal{M} = \{q \in \mathcal{S}^3 : \eta = 0\},$$

which is the connected two-dimensional submanifold of $\mathcal{S}^3$ corresponding to attitudes that are 180° from the desired attitude about some rotation axis. This choice of Lyapunov function naturally leads to the control law $\omega = \phi_2(q) := -\eta\epsilon$. Note that $\phi_2(-q) = \phi_2(q)$. With this control law, we have

$$\left\langle \nabla \widehat{V}_2(q), \tfrac{1}{2} q \otimes \nu(\phi_2(q)) \right\rangle = -\eta^2 \epsilon^\top \epsilon,$$

which is negative on $\mathcal{S}^3 \setminus (\{\pm\mathbf{1}\} \cup \mathcal{M})$. Further analysis shows that $\mathcal{M}$ is a 2-D unstable invariant manifold, and that $\{\pm\mathbf{1}\}$ is attractive from $\mathcal{S}^3 \setminus \mathcal{M}$. Moreover, since the vector field resulting from ϕ_2 vanishes on $\mathcal{M}$, solutions can take an arbitrarily long time to converge to $\pm\mathbf{1}$ as initial conditions are taken closer and closer to $\mathcal{M}$.

To eliminate the undesired equilibrium manifold $\mathcal{M}$, some authors (e.g. [15], [22]–[25], [34]) have used discontinuous feedback motivated by the locally Lipschitz Lyapunov function

$$\widehat{V}_3(q) = 2(1 - |\eta|), \tag{6}$$

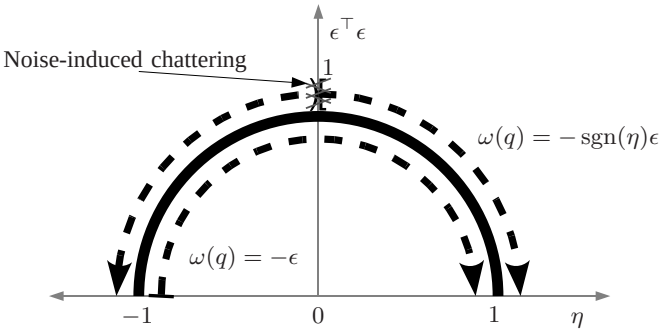

Fig. 1. Quaternion-based attitude control: unwinding produced by continuous control and non-robust global asymptotic stability produced by discontinuous control. Arrows indicate the direction of rotation – towards $\eta = 1$ or $\eta = -1$.

which satisfies $\widehat{V}_3(\pm\mathbf{1}) = 0$ and $\widehat{V}_3(\mathcal{S}^3 \setminus \{\pm\mathbf{1}\}) > 0$. Consider the control law

$$\omega = \phi_3(q) := -\operatorname{sgn}(\eta)\epsilon, \quad \text{where } \operatorname{sgn}(\eta) = \begin{cases} -1 & \eta < 0 \\ 1 & \eta \geq 0. \end{cases} \tag{7}$$

It achieves global asymptotic stability of $\{\pm\mathbf{1}\}$ in the sense of classical solutions to differential equations. However, this stability property is not robust to *arbitrarily* small measurement noise. In fact, [32] appeals to [21, Theorem 2.6] to assert the existence of an arbitrarily small piecewise-constant noise signal that, for initial conditions arbitrarily close to the discontinuity, keeps the state near the discontinuity, (and away from $\{\pm\mathbf{1}\}$) for all time. Note that the discontinuity lies at $\eta = 0$, which corresponds to attitudes that are a 180° rotation from the desired equilibrium.

This point can also be seen through the study of the generalized solutions to the resulting discontinuous system (see [35], [36]). With the control law (7), the closed-loop system becomes

$$\dot{q} = \tfrac{1}{2} q \otimes \nu(-\operatorname{sgn}(\eta)\epsilon) =: f_d(q) \qquad q \in \mathcal{S}^3. \tag{8}$$

We use the following solution concept for solutions to (8).

Definition 3.1 (Carathéodory Solutions): A *Carathéodory solution* to the system $\dot{x} = f(x)$, $x \in \mathbb{R}^n$, on an interval $I \subset \mathbb{R}_{\geq 0}$ is an absolutely continuous function $x : I \to \mathbb{R}^n$ that satisfies $\dot{x}(t) = f(x(t))$ for almost every $t \in I$. Given a measurable function $e : I \to \mathbb{R}^n$, a Carathéodory solution to the system $\dot{x} = f(x + e)$ on I is a function $x : I \to \mathbb{R}^n$ that satisfies $\dot{x}(t) = f(x(t) + e(t))$ for almost all $t \in I$.

The solution obtained by taking the limit of a sequence of Carathéodory solutions $\{x_i\}_{i=1}^\infty$ to $\dot{x} = f(x + e_i)$ with measurable functions $\{e_i\}_{i=1}^\infty$ having the property that, for each t, $\lim_{i \to \infty} e_i(t) = 0$ is called a *Hermes solution* to $\dot{x} = f(x)$; see [35]. The function e_i plays the role of measurement noise. As shown in [35, Corollary 5.6], when f is locally bounded, every Hermes solution to the system $\dot{x} = f(x)$ is a solution to its Krasovskii regularization [37].

The Krasovskii regularization of (8) is given as

$$\dot{q} \in \bar{f}_d(q) := \bigcap_{\delta > 0} \overline{\text{co}} f_d((q + \delta\mathbb{B}) \cap \mathcal{S}^3) \qquad q \in \mathcal{S}^3,$$

where $\overline{\text{co}}$ denotes the closed, convex hull. Let $\rightrightarrows$ denote a set-valued assignment and define $\widehat{\text{sgn}} : \mathbb{R} \rightrightarrows [-1, 1]$ as

$$\widehat{\text{sgn}}(s) = \begin{cases} \text{sgn}(s) & |s| > 0 \\ [-1, 1] & s = 0. \end{cases}$$

Then, the regularized closed-loop system can be written as

$$\dot{q} \in \tfrac{1}{2} q \otimes \nu\left(-\widehat{\text{sgn}}(\eta)\epsilon\right) \qquad q \in \mathcal{S}^3.$$

For every $q \in \mathcal{M}$, it follows that $0 \in \bar{f}_d(q)$. Thus, $\mathcal{M} := \{q \in \mathcal{S}^3 : \eta = 0\}$ is an equilibrium set of the regularized system. The equivalence between Krasovskii and Hermes solutions indicates that when measurement noise is present, solutions to the unregularized system can approximate such an equilibrium solution.

Theorem 3.2: Let $\phi_3(q) = -\text{sgn}(\eta)\epsilon$. Then, for each $\alpha > 0$ and each $q_0 \in (\mathcal{M} + \alpha\mathbb{B}) \cap \mathcal{S}^3$, there exist a measurable function $e : [0, \infty) \to \alpha\mathbb{B}$ and a Carathéodory solution $q : [0, \infty) \to \mathcal{S}^3$ to $\dot{q} = \frac{1}{2} q \otimes \nu\left(\phi_3(q + e)\right)$ satisfying $q(0) = q_0$ and $q(t) \in (\mathcal{M} + \alpha\mathbb{B}) \cap \mathcal{S}^3$ for all $t \in [0, \infty)$.

Proof: This result can be seen as a consequence of [35, Corollary 5.6] or [21, Theorem 2.6]; however, we provide an alternative proof by explicitly constructing a noise signal e. Let $\alpha > 0$ and define e to be the function of the state $e = (-\alpha \,\text{sgn}(\eta), 0)$. Then, it follows that

$$\dot{q} = \begin{cases} \frac{1}{2} q \otimes \nu(\text{sgn}(\eta)\epsilon) & 0 \leq |\eta| \leq \alpha \\ \frac{1}{2} q \otimes \nu(-\text{sgn}(\eta)\epsilon) & |\eta| > \alpha. \end{cases}$$

Solutions to this system yield a measurable function $e : [0, \infty) \to \alpha\mathbb{B}$. We define $\widehat{V}_{\mathcal{M}}(q) = \eta^2$, which has the property that $\widehat{V}_{\mathcal{M}}(\mathcal{S}^3 \setminus \mathcal{M}) > 0$ and $\widehat{V}_{\mathcal{M}}(\mathcal{M}) = 0$. It follows that, for $0 \leq |\eta| \leq \alpha$,

$$\left\langle \nabla \widehat{V}_{\mathcal{M}}(q), \tfrac{1}{2} q \otimes \nu(-\text{sgn}(\eta - \alpha \,\text{sgn}(\eta))\epsilon) \right\rangle = -|\eta| \epsilon^\top \epsilon.$$

Standard Lyapunov theory yields the desired result. ■

Interestingly, this result directly contradicts the assertion of [24] that defining sgn without a zero value at zero, as we have in (7), avoids the regularization-induced equilibrium.

While some might dismiss this development since the regularization-induced equilibrium set has measure zero in the space of unit quaternions, the fact remains that such a discontinuous control produces global asymptotic stability without robustness. One can imagine that oscillating noise could, at the very least, *degrade* performance as a fickle discontinuous feedback changes its "mind" on which way to rotate. Referring to Fig. 1, one can visualize how noise affecting the measurement of η can cause chattering at the discontinuity ($\eta = 0$). We now show how one can add decisiveness with a hysteretic memory state encapsulated in a hybrid feedback.

To solve the various issues in the control laws above, we propose the strategy suggested in Figure 2: a *dynamic* feedback that uses a memory state to select which pole of $\mathcal{S}^3$ to regulate in a *hysteretic* fashion. Let $\delta \in (0, 1)$ denote the hysteresis half-width and let $\overline{\text{sgn}} : \mathbb{R} \rightrightarrows \{-1, 1\}$ be the outer

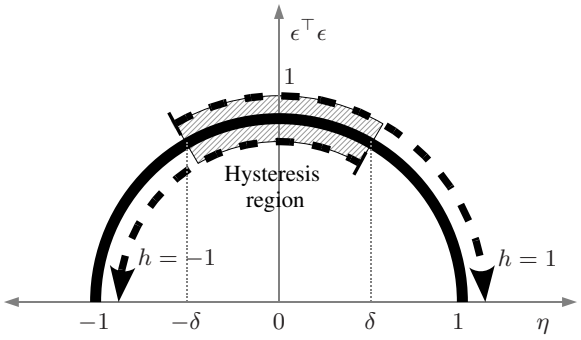

Fig. 2. Hysteretic regulation of unit quaternions to the set $\{\pm\mathbf{1}\}$. The state space for η and $\epsilon^\top \epsilon$ is represented by the semicircle. The value of h determines if $q = (\eta, \epsilon)$ should be regulated to $\mathbf{1}$ or $-\mathbf{1}$. The parameter δ determines the hysteresis half-width.

semicontinuous set-valued map

$$\overline{\text{sgn}}(s) = \begin{cases} \text{sgn}(s) & |s| > 0 \\ \{-1, 1\} & s = 0. \end{cases} \tag{9}$$

Consider the feedback $\omega = \phi_4(q, h) = -h\epsilon$, where $h \in \{-1, 1\}$ and the dynamics of h are

$$\begin{aligned} \dot{h} &= 0 && \text{when } (q, h) \in \{h\eta \geq -\delta\} \\ h^+ &\in \overline{\text{sgn}}(\eta) && \text{when } (q, h) \in \{h\eta \leq -\delta\}, \end{aligned}$$

where h^+ denotes the value of the logic variable after being updated. This is a hybrid feedback in which h selects the desired rotation direction to move q to either $+\mathbf{1}$ or $-\mathbf{1}$. The inequalities dictating whether h remains constant or changes value are designed to switch h only when a "significant" sign mismatch occurs between η and h. Note that when $h\eta \geq 0$, the feedback $-h\epsilon$ is pulling in the direction of the shortest rotation to align q with $\pm\mathbf{1}$. On the other hand, when $h\eta \leq 0$, the feedback is pulling in the direction of a longer rotation. Hence, the desired direction of rotation changes only when there is a significant benefit in switching it, where "significant" is defined precisely by the selection of δ.

The hybrid feedback ϕ_4 generalizes the feedbacks ϕ_1 and ϕ_3, as $\phi_4(q, \text{sgn}(\eta)) = \phi_3(q)$ and $\phi_4(q, h) = h\phi_1(q)$. The hysteresis width δ manages a trade-off between robustness to measurement noise and a small amount of hysteresis-induced inefficiency. When $\delta \geq 1$, the value of the logic variable cannot change and our strategy reduces to a static feedback that induces unwinding. When $\delta = 0$, the resulting control becomes discontinuous.

This similarity is also present in the Lyapunov analysis. For notational convenience, we let

$$f(q, h) = \begin{bmatrix} \frac{1}{2} q \otimes \nu(\phi_4(q, h)) \\ 0 \end{bmatrix} \quad g(q, h) = \begin{bmatrix} q \\ \overline{\text{sgn}}(\eta) \end{bmatrix}$$

Now, we consider the Lyapunov function

$$\widehat{V}_4(q, h) = 2(1 - h\eta) = \widehat{V}_1(hq),$$

which satisfies $\widehat{V}_4(q, h) = 0$ if and only if $q = h\mathbf{1}$, while it is positive otherwise. Since $h^2 = 1$, it follows that

$$\left\langle \nabla \widehat{V}_4(q, h), f(q, h) \right\rangle = -\epsilon^\top \epsilon,$$

which is negative whenever $h\eta \geq -\delta$ and $q \neq h\mathbf{1}$. That is, $\widehat{V}_4$ decreases along flows of the closed-loop system. Furthermore, we have that

$$\widehat{V}_4(g(q,h)) - \widehat{V}_4(q,h) = 4h\eta,$$

which is negative whenever $h\eta \leq -\delta$, that is, $\widehat{V}_4$ decreases over jumps of the closed-loop system. This analysis implies that the compact and invariant set $\mathcal{A} = \{(q,h) \in \mathcal{S}^3 \times \{-1,1\} \ : \ q = h\mathbf{1}\}$ is globally asymptotically stable for the closed-loop system since $\widehat{V}_4$ is strictly decreasing along all trajectories, except of those starting from $\mathcal{A}$. Finally, we note that the hysteresis makes the scenario described in Theorem 3.2 impossible. In the coming sections, we will find that these ideas extend naturally to the dynamic setting where ω is a state variable and torque is an input.

As a final remark, the correctness of any convergence or stability result written for rigid body attitude control using quaternions fundamentally depends on using a measurement of q that satisfies the quaternion kinematic equation (4). Here, we quote the seminal paper [16].

> "In many quaternion extraction algorithms, the sign of η is arbitrarily chosen positive. This approach is not used here, instead, the sign ambiguity is resolved by choosing the one that satisfies the associated kinematic differential equation. In implementation, this would probably imply keeping some immediate past values of the quaternion."

We note that additionally, such a discontinuous quaternion selection method is inherently non-global, as η can easily be zero (destroying a main purpose of quaternion use). Instead, as the quotation above suggests, properly implemented quaternion-based control laws are *inherently dynamic* and require an extra quaternion memory state to properly "extract" the measurement of q from a measurement of R. We assume that this mechanism is working in the background and omit it from the analysis.

IV. Tracking Error Dynamics

The tracking objective is to design τ so that R and ω asymptotically track a desired bounded reference trajectory. To pose this tracking problem in terms of a compact attractor for an autonomous system, we utilize an exogenous system to generate any useful reference trajectory. Let $M > 0$ and $\Omega \subset \mathbb{R}^3$ be compact. Then, we generate such desired reference trajectories with the system

$$\left.\begin{aligned} \dot{R}_d &= R_d S(\omega_d) \\ \dot{\omega}_d &\in M\mathbb{B} \end{aligned}\right\} \qquad (R_d, \omega_d) \in SO(3) \times \Omega, \tag{10}$$

where $M\mathbb{B}$ denotes the closed ball of radius M. Since $0 \in M\mathbb{B}$, $SO(3) \times \Omega$ is always viable (see [38]). Then, since $SO(3) \times \Omega$ is compact, every maximal solution (i.e., it is not a proper truncation of another solution) to (10) is complete (i.e., has an unbounded domain–see, e.g., [39, Proposition 2.4]). Additionally, any possible solution component ω_d of (10) is Lipschitz continuous with Lipschitz constant M, but not necessarily differentiable. This formulation also allows for non-periodic ω_d and includes the regulation problem as well. We will assume that $\dot{\omega}_d$ can be measured. We note that the inclusion formulation of the generator system (10) is autonomous; hence, invariance principles for hybrid systems can be used to assert convergence of solutions.

To express the difference between the reference trajectory, (R_d, ω_d), and the actual rigid body trajectory, (R, ω), we employ a common coordinate transformation that resolves the angular velocity error in the body frame (see [5], [7], [20], [23], [40], [41]). In this direction, we define the attitude error coordinates $\bar{R} = R_d^\top R \in SO(3)$. Using the property that $x \mapsto S(x)$ is linear and that for every $x \in \mathbb{R}^3$ and $R \in SO(3)$, $R^\top S(x) R = S(R^\top x)$, it follows that the attitude error system evolves according to

$$\dot{\bar{R}} = \bar{R} S(\omega - \bar{R}^\top \omega_d). \tag{11}$$

We define

$$\bar{\omega}_d = \bar{R}^\top \omega_d, \qquad \bar{\omega} = \omega - \bar{\omega}_d. \tag{12}$$

Then, defining

$$\Sigma(\bar{\omega}, \bar{\omega}_d) := S(\mathcal{J}\bar{\omega}) + S(\mathcal{J}\bar{\omega}_d) - (S(\bar{\omega}_d)\mathcal{J} + \mathcal{J}S(\bar{\omega}_d)),$$

following [20], [23], [40], [41] yields the error dynamics

$$\begin{aligned} \dot{\bar{R}} &= \bar{R} S(\bar{\omega}) \\ \mathcal{J}\dot{\bar{\omega}} &= \Sigma(\bar{\omega}, \bar{\omega}_d)\bar{\omega} - S(\bar{\omega}_d)\mathcal{J}\bar{\omega}_d - \mathcal{J}\bar{R}^\top \dot{\omega}_d + \tau \end{aligned} \tag{13}$$

The salient features of this transformation are that $\Sigma(\bar{\omega}, \bar{\omega}_d)$ is skew symmetric for every value of its argument and that, assuming the inertia matrix $\mathcal{J}$ is known, $S(\bar{\omega}_d)\mathcal{J}\bar{\omega}_d$ and $\mathcal{J}\bar{R}^\top \dot{\omega}_d$ can be inferred through measurement of R.

The error system (13) can be expressed in terms of unit quaternions as well. Letting $q_d = (\eta_d, \epsilon_d) \in \mathcal{S}^3$ denote the desired quaternion, where $\dot{q}_d = \frac{1}{2} q_d \otimes \nu(\omega_d)$, we define the tracking error quaternion as $\bar{q} = q_d^{-1} \otimes q = (\bar{\eta}, \bar{\epsilon})$. Then, performing the same coordinate transformation, $\bar{\omega}_d = \mathcal{R}(\bar{q})^\top \omega_d$, it follows that

$$\dot{\bar{q}} = \tfrac{1}{2} \bar{q} \otimes \nu(\bar{\omega}). \tag{14}$$

We define the *feedforward* torque term as

$$\tau_{ff}(\bar{q}, \bar{\omega}_d, \dot{\omega}_d) = \mathcal{J}\mathcal{R}(\bar{q})^\top \dot{\omega}_d + S(\bar{\omega}_d)\mathcal{J}\bar{\omega}_d. \tag{15}$$

Finally, we let $x_p = (q, \omega, q_d, \omega_d)$, $\bar{x}_p = (\bar{q}, \bar{\omega}, q_d, \omega_d)$, and $\mathcal{X}_p = \mathcal{S}^3 \times \mathbb{R}^3 \times \mathcal{S}^3 \times \Omega$, so that, with this formulation, the tracking objective is to robustly, globally asymptotically stabilize the compact set

$$\begin{aligned} \mathcal{A}_p &= \{\bar{x}_p \in \mathcal{X}_p : \mathcal{R}(\bar{q}) = I, \ \bar{\omega} = 0\} \\ &= \{\bar{x}_p \in \mathcal{X}_p : \bar{q} = \pm\mathbf{1}, \ \bar{\omega} = 0\} \end{aligned} \tag{16}$$

for the autonomous system

$$\dot{\bar{x}}_p = \begin{bmatrix} \dot{\bar{q}} \\ \dot{\bar{\omega}} \\ \dot{q}_d \\ \dot{\omega}_d \end{bmatrix} \in F_p(\bar{x}_p, \tau) := \begin{bmatrix} \frac{1}{2}\bar{q} \otimes \nu(\bar{\omega}) \\ f_\omega(\bar{x}_p, \tau) \\ \frac{1}{2} q_d \otimes \nu(\omega_d) \\ M\mathbb{B} \end{bmatrix} \qquad \bar{x}_p \in \mathcal{X}_p, \tag{17}$$

where

$$f_\omega(\bar{x}_p, \tau) = \mathcal{J}^{-1} \left(\Sigma(\bar{\omega}, \bar{\omega}_d)\bar{\omega} - \tau_{ff}(\bar{q}, \bar{\omega}_d, \dot{\omega}_d) + \tau \right).$$

Preprint submitted to IEEE Transactions on Automatic Control. Received: January 18, 2011 20:37:59 PST

V. Attitude Tracking Control

We now consider three attitude tracking control scenarios:

1) measurements of q and ω are available;
2) only measurements of q are available;
3) measurements of q and $\omega + b$ are available, where b is an unknown constant bias.

Our solution to 1) is an extension of [32] and the hybrid feedback of Section III to the tracking problem, for which we employ the error coordinates of Section IV and feedforward compensation. It uses a single binary logic variable as described in Fig. 2 to achieve global asymptotic attitude tracking that is robust to measurement noise.

To solve 2), we build on our solution to 1) by employing the results of [20] that use an extra quaternion filter to provide damping that would otherwise be accomplished by negative feedback of angular-velocity error terms. In [20], a Lyapunov function based on (5) is used for both the tracking error quaternion and the extra quaternion filter state. We remove the unwinding caused by this choice of Lyapunov function by introducing another binary logic variable for the quaternion filter and implementing the ideas in Fig. 2.

Finally, our solution to 3) uses the ideas of [23], which, based on the observer design of [22], employ a coupled quaternion filter similar to the one in [20] and a bias observer to achieve asymptotic tracking. Unlike [20], the works [23] and [22] use a Lyapunov function based on (6) and its resulting non-robust discontinuous control to avoid unwinding. Here, we directly build on our solution to 2) by adding a bias observer. In fact, our solution to 2) can be seen as a special case of our solution to 3) without the bias observer and extra feedback term.

To summarize, our proposed controllers are dynamic and employ hysteretically switched logic variables for each quaternion error state. The solutions to 2) and 3) employ an additional quaternion filter to achieve damping and the solution to 3) uses an additional bias observer. We note that 2) has been solved using a linear attitude filter in [19] and [42]. It may be possible to extend these methods to solve 3). Because the present paper is primarily concerned with the quaternion representation, we have chosen to employ quaternion filters, although the use of a linear filter would obviate the need for an additional logic variable.

In what follows, we will make use of comparison functions and a function that removes energy from the system. A continuous function $\gamma : \mathbb{R}_{\geq 0} \to \mathbb{R}_{\geq 0}$ is said to be *class-$\mathcal{K}$* if $\gamma(0) = 0$ and it is strictly increasing. A continuous function $\beta : \mathbb{R}_{\geq 0} \to \mathbb{R}_{\geq 0}$ is said to be *class-$\mathcal{KL}$* if for each fixed r, the map $s \mapsto \beta(s, r)$ is class-$\mathcal{K}$ and if for each fixed s, the map $r \mapsto \beta(s, r)$ is decreasing and $\lim_{r\to\infty} \beta(s, r) = 0$. A continuous function $\Phi : \mathbb{R}^n \to \mathbb{R}^n$ is *strongly passive* if there exist class-$\mathcal{K}$ functions γ_i, $i \in \{1, 2\}$, such that $\gamma_1(\|\omega\|) \leq \omega^\top \Phi(\omega) \leq \gamma_2(\|\omega\|)$ for all $\omega \in \mathbb{R}^n$. Finally, we work within the hybrid systems framework of [43] in which a hybrid system is denoted as $\mathcal{H} = (F, G, C, D)$ and given by

$$\mathcal{H} \begin{cases} \dot{x} \in F(x) & x \in C \\ x^+ \in G(x) & x \in D, \end{cases}$$

where $F : \mathbb{R}^n \rightrightarrows \mathbb{R}^n$ is the *flow map* governing continuous evolution of the state x on the *flow set* C, while $G : \mathbb{R}^n \rightrightarrows \mathbb{R}^n$ is the *jump map* governing the discrete evolution of the state on the *jump set* D. For details, see [39], [43].

In the following sections, we will make several divisions of the state space by notation to precisely indicate where measurement noise enters the closed-loop systems, As a notational guide, a bar or tilde embellishment indicates an error state, a numbered subscript indicates the problem number (e.g. $i = 1$: full state measurements), a p subscript indicates the plant state, a c subscript indicates the controller state, and a subscript k indicates the "known" states.

A. Full state measurements

We assume the output of the system (17) is given as

$$y_1 = (q, \omega). \tag{18}$$

The proposed controller has a single state, $\bar{h} \in \{-1, 1\}$, so we partition the state space as follows. We define the controller state and state space as $x_{c,1} := \bar{h} \in \mathcal{X}_{c,1} := \{-1, 1\}$. For consistency in indexing and notation throughout the following sections, we let $x_{p,1} := x_p$, $\bar{x}_{p,1} := \bar{x}_p$, $\mathcal{X}_{p,1} := \mathcal{X}_p$, $\bar{x}_{c,1} := \bar{h}$, $x_1 := (x_{p,1}, x_{c,1})$, $\bar{x}_1 := (\bar{x}_{p,1}, \bar{x}_{c,1})$, and $\mathcal{X}_1 := \mathcal{X}_{p,1} \times \mathcal{X}_{c,1}$. Finally, we let $x_{k,1} = (q_d, \omega_d, x_{c,1})$.

The goal is to globally asymptotically stabilize the set

$$\mathcal{A}_1 = \left\{ \bar{x}_1 \in \mathcal{X}_1 : \bar{q} = \bar{h}\mathbf{1},\ \bar{\omega} = 0 \right\}. \tag{19}$$

That is, q should be regulated to $\bar{h} q_d$ and ω should be regulated to ω_d. Note that $\mathrm{Proj}_{\mathcal{X}_p} \mathcal{A}_1 = \mathcal{A}_p$, where $\mathrm{Proj}_Y X$ is the projection of the set X onto the set Y.

Given a gain $\bar{c} > 0$, a strongly passive function $\Phi : \mathbb{R}^3 \to \mathbb{R}^3$, and $\delta \in (0, 1)$, our hybrid controller is

$$\begin{array}{ll} \dot{\bar{h}} = 0 & \bar{x}_1 \in C_1 := \{\bar{x}_1 \in \mathcal{X}_1 : \bar{h}\bar{\eta} \geq -\delta\} \\ \bar{h}^+ \in \overline{\mathrm{sgn}}(u_1) & \bar{x}_1 \in D_1 := \{\bar{x}_1 \in \mathcal{X}_1 : \bar{h}\bar{\eta} \leq -\delta\}, \end{array} \tag{20}$$

where the vector of inputs $U_1 = (\tau, u_1)$ is specified by defining

$$\tau_{fb,1}(y_1, x_{k,1}) = -\bar{c}\bar{h}\bar{\epsilon} - \Phi(\bar{\omega}), \quad \kappa_1(y_1, x_{k,1}) = \bar{\eta}, \tag{21}$$

and setting $U_1 = \mathcal{K}_1 = (\tau_{ff} + \tau_{fb,1}, \kappa_1)$.

The torque feedback term $\tau_{fb,1}$ is quite similar to other works. The "proportional" term $-\bar{c}\bar{h}\bar{\epsilon}$ essentially implements a spring force that pulls the rigid body along the axis of rotation. As discussed in Section III, $\bar{h}$ determines the orientation of the spring force and that because of the hysteresis, this spring force may sometimes pull in the direction of the longer rotation. Damping is provided by $-\Phi(\bar{\omega})$. The whole torque input is comprised of the feedback part $\tau_{fb,1}$ and the feedforward part $\tau_{ff,1}$, which is model dependent when either $\bar{\omega}_d$ or $\dot{\omega}_d$ is nonzero.

B. Only attitude measurements available

Here, we assume the output of the system (17) is given as

$$y_2 = q. \tag{22}$$

We append two states to the hybrid controller outlined in Section V-A: a quaternion filter state, $\hat{q} \in \mathcal{S}^3$, and an

accompanying hysteresis variable, $\tilde{h}$. The control law in this instance is additionally parametrized by a gain $\tilde{c} > 0$ and a matrix gain $\tilde{K} = \tilde{K}^\top > 0$. The state and state space of the controller is $x_{c,2} = (x_{c,1}, \tilde{h}, \hat{q}) \in \mathcal{X}_{c,2} := \mathcal{X}_{c,1} \times \{-1, 1\} \times \mathcal{S}^3$. The quaternion error between $\hat{q}$ and $\bar{q}$ is

$$\tilde{q} = \hat{q}^{-1} \otimes \bar{q}. \tag{23}$$

Now, we let $x_{p,2} := x_{p,1}$, $\mathcal{X}_{p,2} := \mathcal{X}_{p,1}$, $\bar{x}_{c,2} := (\bar{x}_{c,1}, \tilde{h}, \tilde{q})$, $x_2 := (x_{p,2}, x_{c,2})$, $\bar{x}_2 := (\bar{x}_{p,2}, \bar{x}_{c,2})$, $\mathcal{X}_2 = \mathcal{X}_{p,2} \times \mathcal{X}_{c,2}$, and finally, $x_{k,2} = (q_d, \omega_d, x_{c,2})$. Now, we can state the goal of our proposed controller as globally asymptotically stabilizing the compact set

$$\mathcal{A}_2 = \{\bar{x}_2 \in \mathcal{X}_2 : \bar{x}_1 \in \mathcal{A}_1,\ \tilde{q} = \tilde{h}\mathbf{1}\}. \tag{24}$$

As before, $\tilde{h}$ decides to regulate $\hat{q}$ to $\bar{q}$ or $-\bar{q}$ and we have $\mathrm{Proj}_{\mathcal{X}_p} \mathcal{A}_2 = \mathcal{A}_p$, where $\mathcal{A}_p$ was defined in (16).

For this task, we propose the hybrid controller (again expressed in terms of inputs)

$$\begin{bmatrix} \dot{\bar{h}} \\ \dot{\tilde{h}} \\ \dot{\hat{q}} \end{bmatrix} = \begin{bmatrix} 0 \\ 0 \\ \frac{1}{2}\hat{q} \otimes \nu(u_2) \end{bmatrix} \quad \bar{x}_2 \in C_2 := \{\bar{x}_2 \in \mathcal{X}_2 : \bar{h}\bar{\eta} \geq -\delta \text{ and } \tilde{h}\tilde{\eta} \geq -\delta\}$$
$$\begin{bmatrix} \bar{h}^+ \\ \tilde{h}^+ \\ \hat{q}^+ \end{bmatrix} \in \begin{bmatrix} \overline{\mathrm{sgn}}(u_1) \\ \overline{\mathrm{sgn}}(u_3) \\ \hat{q} \end{bmatrix} \quad \bar{x}_2 \in D_2 := \{\bar{x}_2 \in \mathcal{X}_2 : \bar{h}\bar{\eta} \leq -\delta \text{ or } \tilde{h}\tilde{\eta} \leq -\delta\}, \tag{25}$$

where the vector of inputs $U_2 = (U_1, u_2, u_3)$ is defined by

$$\tau_{fb,2}(y_2, x_{k,2}) := -\bar{c}\bar{h}\bar{\epsilon} - \tilde{c}\tilde{h}\tilde{\epsilon} \quad \kappa_2(y_2, x_{k,2}) := \tilde{h}\tilde{K}\tilde{\epsilon} \quad \kappa_3(y_2, x_{k,2}) := \tilde{\eta}, \tag{26}$$

and setting $U_2 = \mathcal{K}_2 := (\tau_{ff} + \tau_{fb,2}, \kappa_1, \kappa_2, \kappa_3)$. Here, much is the same as [20], where the extra quaternion filter exploits passivity to introduce damping. The primary and crucial difference between [20] and our approach above is our addition of logic variables for each quaternion state.

Compared to the full state feedback controller of Section V-A, the quaternion filter state $\hat{q}$ and logic variable $\tilde{h}$ introduced in this design necessitates some additional structure in the flow and jump sets. Conditions are included in the jump and flow sets to update $\tilde{h}$ when there is a significant amount of sign mismatch between $\tilde{\eta}$ and $\tilde{h}$, and otherwise, keep it constant. Note that (25) guarantees that, when *either* jump condition is met, *both* logic variables $\bar{h}$ and $\tilde{h}$ are reset to the sign of their respective η's.

C. Biased angular velocity measurements

In this section, we append a constant bias state, $b \in \Omega \subset \mathbb{R}^3$ to the plant: $x_{p,3} := (x_{p,2}, b) \in \mathcal{X}_{p,3} := \mathcal{X}_{p,2} \times \Omega$ with dynamics $\dot{b} = 0$. We assume the output of (17) is given as

$$y_3 = (q, \omega + b). \tag{27}$$

We append a bias observer state, $\hat{b} \in \mathbb{R}^3$, to the controller state as $x_{c,3} := (x_{c,2}, \hat{b}) \in \mathcal{X}_{c,3} := \mathcal{X}_{c,2} \times \mathbb{R}^3$. We define the bias observer error as

$$\tilde{b} = \hat{b} - b. \tag{28}$$

Now, we let $\bar{x}_{c,3} := (\bar{x}_{c,2}, \tilde{b})$, $x_3 := (x_{p,3}, x_{c,3})$, $\bar{x}_3 := (\bar{x}_{p,3}, \bar{x}_{c,3})$, $\mathcal{X}_3 = \mathcal{X}_{p,3} \times \mathcal{X}_{c,3}$, and finally, $x_{k,3} = (q_d, \omega_d, x_{c,3})$. Our goal is to stabilize the compact set

$$\mathcal{A}_3 = \{\bar{x}_3 \in \mathcal{X}_3 : \bar{x}_2 \in \mathcal{A}_2,\ \tilde{b} = 0\}, \tag{29}$$

which satisfies $\mathrm{Proj}_{\mathcal{X}_p} \mathcal{A}_3 = \mathcal{A}_p$.

Let $\hat{\omega} = \omega + b - \hat{b}$ denote the estimate of the unbiased angular velocity measurement. Then, for this task, we propose the hybrid controller

$$\begin{bmatrix} \dot{\bar{h}} \\ \dot{\tilde{h}} \\ \dot{\hat{q}} \\ \dot{\hat{b}} \end{bmatrix} = \begin{bmatrix} 0 \\ 0 \\ \frac{1}{2}\hat{q} \otimes \nu(u_2) \\ u_4 \end{bmatrix} \quad \bar{x}_3 \in C_3 := \{\bar{x}_3 \in \mathcal{X}_3 : \bar{h}\bar{\eta} \geq -\delta \text{ and } \tilde{h}\tilde{\eta} \geq -\delta\}$$
$$\begin{bmatrix} \bar{h}^+ \\ \tilde{h}^+ \\ \hat{q}^+ \\ \hat{b}^+ \end{bmatrix} \in \begin{bmatrix} \overline{\mathrm{sgn}}(u_1) \\ \overline{\mathrm{sgn}}(u_3) \\ \hat{q} \\ \hat{b} \end{bmatrix} \quad \bar{x}_3 \in D_3 := \{\bar{x}_3 \in \mathcal{X}_3 : \bar{h}\bar{\eta} \leq -\delta \text{ or } \tilde{h}\tilde{\eta} \leq -\delta\} \tag{30}$$

where the vector of inputs $U_3 = (U_2, u_4)$ is defined by

$$\begin{aligned} \tau_{fb,3}(y_3, x_{k,3}) &:= -\bar{c}\bar{h}\bar{\epsilon} - \tilde{c}\tilde{h}\tilde{\epsilon} - \Phi(\hat{\omega} - \bar{\omega}_d), \\ \kappa_4(y_3, x_{k,3}) &:= \Phi(\hat{\omega} - \bar{\omega}_d) \end{aligned} \tag{31}$$

and setting $U_3 = \mathcal{K}_3 := (\tau_{ff} + \tau_{fb,3}, \kappa_1, \kappa_2, \kappa_3, \kappa_4)$. Here, the estimated value of $\bar{\omega}$ is used in certainty equivalence fashion. The term $\Phi(\hat{\omega} - \bar{\omega}_d)$ in κ_4 acts to estimate b by exploiting the passivity of feedback loops with $\tilde{b}$, $\bar{\omega}$ and $\tilde{q}$. The addition of the bias state and its observer requires no additional complexity in terms of logic variables (and accompanying flow and jump conditions) over the output feedback case considered in Section V-B. This is due to the fact that the bias and its estimate evolve in $\mathbb{R}^3$, free of topological constraints.

D. Closed-loop error system and main results

In this section, we combine the results of previous sections and prove global asymptotic stability of $\mathcal{A}_i$ for the i^{th} closed-loop error system, $i \in \{1, 2, 3\}$. Below, we show the open-loop error system for $i = 1, 2, 3$ by displaying the evolution of all error states with nontrivial dynamics (i.e., $\dot{x} \neq 0$, $x^+ \neq x$). We slightly abuse notation to save space by writing $\bar{x}_i \in C_i$, even when the states listed below may not belong to the state space of which C_i is a closed subset. In terms of the input vectors U_i, the error system is

$$\underbrace{\begin{aligned} \dot{\bar{q}} &= \tfrac{1}{2}\bar{q} \otimes \nu(\bar{\omega}) \\ \mathcal{J}\dot{\bar{\omega}} &= \Sigma(\bar{\omega}, \bar{\omega}_d)\bar{\omega} - \tau_{ff}(\bar{q}, \bar{\omega}_d, \dot{\bar{\omega}}_d) + \tau \\ \dot{q}_d &= \tfrac{1}{2} q_d \otimes \nu(\omega_d) \\ \dot{\omega}_d &\in M\mathbb{B} \\ \dot{\hat{q}} &= \tfrac{1}{2}\tilde{q} \otimes \nu(\bar{\omega} - \mathcal{R}(\tilde{q})^\top u_2) \\ \dot{\tilde{b}} &= u_4 \end{aligned}}_{\bar{x}_i \in C_i} \qquad \underbrace{\begin{aligned} \bar{h}^+ &\in \overline{\mathrm{sgn}}(u_1) \\ \tilde{h}^+ &\in \overline{\mathrm{sgn}}(u_3) \end{aligned}}_{\bar{x}_i \in D_i,} \tag{32}$$

which we abbreviate as

$$\mathcal{H}_i(U_i) \begin{cases} \dot{\bar{x}}_i \in F_i(\bar{x}_i, U_i) & \bar{x}_i \in C_i \\ \bar{x}_i^+ \in G_i(\bar{x}_i, U_i) & \bar{x}_i \in D_i. \end{cases} \tag{33}$$

Preprint submitted to IEEE Transactions on Automatic Control. Received: January 18, 2011 20:37:59 PST

We note that the evolution for $\tilde{b}$ is calculated trivially from the definition $\tilde{b} = \hat{b} - b$ and that the evolution for $\tilde{q}$ can be derived in much the same way as $\bar{q}$ in (11), (12), and (14).

Closing the loop by setting $U_i = \mathcal{K}_i(y_i, x_{k,i}, \dot{\omega}_d)$, we have

$$\begin{aligned} &\dot{\bar{x}}_p \in F_p(\bar{x}_p, \tau_{ff} + \tau_{fb,i}) \\ &\dot{\tilde{q}} = \tfrac{1}{2}\tilde{q} \otimes \nu\left(\bar{\omega} - \mathcal{R}(\tilde{q})^\top \tilde{K}\tilde{\epsilon}\right) \qquad \bar{h}^+ \in \overline{\mathrm{sgn}}(\bar{\eta}) \\ &\dot{\tilde{b}} = \Phi(\hat{\omega} - \bar{\omega}_d) \qquad\qquad\qquad \tilde{h}^+ \in \overline{\mathrm{sgn}}(\tilde{\eta}) \\ &\underbrace{\qquad\qquad\qquad\qquad}_{\bar{x}_i \in C_i} \qquad\qquad \underbrace{\qquad\qquad}_{\bar{x}_i \in D_i} \end{aligned} \tag{34}$$

which we abbreviate by defining $\overline{\mathcal{H}}_i = (\overline{F}_i, \overline{G}_i, C_i, D_i) := \mathcal{H}_i(\mathcal{K}_i)$. Before commencing our stability analysis, we note that our closed-loop systems satisfy the following properties.

Lemma 5.1: For $i = 1, 2, 3$, the closed-loop system $\overline{\mathcal{H}}_i$ corresponding to (34) *satisfies the following properties*[1]*:*

(A1) *C_i and D_i are closed sets.*

(A2) *$\overline{F}_i : \mathbb{R}^n \rightrightarrows \mathbb{R}^n$ is outer semicontinuous, locally bounded, convex-valued, and $\overline{F}_i(x) \neq \emptyset$ for all $x \in C_i$.*

(A3) *$\overline{G}_i : \mathbb{R}^n \rightrightarrows \mathbb{R}^n$ is outer semicontinuous, locally bounded, and $\overline{G}_i(x) \neq \emptyset$ for all $x \in D_i$.*

Proof: The following statements hold for $i \in \{1, 2, 3\}$. The sets C_i and D_i are obviously closed by inspection. The flow equation for every state except for ω_d is continuous and locally bounded. Since $M\mathbb{B}$ has no dependence on $\bar{x}_i$, it is outer semicontinuous. Moreover, $M\mathbb{B}$ is convex and bounded. $\overline{G}_i(\bar{x}_i)$ is nonempty for every $\bar{x}_i \in D_i$. Moreover, since $s \mapsto \overline{\mathrm{sgn}}(s)$ is outer-semicontinuous, $\overline{G}_i(\bar{x}_i)$ is outer-semicontinuous for all $\bar{x}_i \in D_i$. ∎

Our analysis is based on Lyapunov's method and the functions $V_i : \mathcal{X}_i \to \mathbb{R}_{\geq 0}$, defined as

$$V_1(\bar{x}_1) = 2\bar{c}(1 - \bar{h}\bar{\eta}) + \tfrac{1}{2}\bar{\omega}^\top \mathcal{J}\bar{\omega} \tag{35a}$$

$$V_2(\bar{x}_2) = V_1(\bar{x}_1) + 2\tilde{c}(1 - \tilde{h}\tilde{\eta}) \tag{35b}$$

$$V_3(\bar{x}_3) = V_2(\bar{x}_2) + \tfrac{1}{2}\tilde{b}^\top \tilde{b} \tag{35c}$$

Theorem 5.2: Let $\bar{c} > 0$, $\tilde{c} > 0$, $\tilde{K} = \tilde{K}^\top > 0$, $\delta \in (0, 1)$, and let $\Phi : \mathbb{R}^3 \to \mathbb{R}^3$ be strongly passive. Then, the compact set $\mathcal{A}_i$ ((19), (24), (29)*) is globally asymptotically stable for the closed-loop hybrid system $\overline{\mathcal{H}}_i$* (34)*, for each $i \in \{1, 2, 3\}$.*

Proof: Consider the functions $V_i : \mathcal{X}_i \to \mathbb{R}_{\geq 0}$ in (35). For $i = 1, 2, 3$, V_i satisfies $V_i(\mathcal{X}_i \setminus \mathcal{A}_i) > 0$, $V_i(\mathcal{A}_i) = 0$, and for any $a > 0$, the set $\{\bar{x}_i \in \mathcal{X}_i : V(\bar{x}_i) \leq a\}$ is compact. Let $\sigma = -\tau_{ff} + \bar{c}\bar{h}\bar{\epsilon} + \tilde{c}\tilde{h}\tilde{\epsilon} + \tau$. Now, written in terms of the input vector U_i, we have that

$$\left\langle \nabla V_i(\bar{x}_i), F_i(\bar{x}_i, U_i) \right\rangle = \begin{cases} \bar{\omega}^\top \sigma & i = 1 \\ -\tilde{c}\tilde{h}\tilde{\epsilon}^\top u_2 + \bar{\omega}^\top \sigma & i = 2 \\ -\tilde{c}\tilde{h}\tilde{\epsilon}^\top u_2 + \bar{\omega}^\top \sigma + \tilde{b}^\top u_3 & i = 3. \end{cases} \tag{36}$$

To see this, we note from (4) and (14) that $2\bar{c}(1 - \bar{h}\dot{\bar{\eta}}) = \bar{c}\bar{h}\bar{\omega}^\top \bar{\epsilon}$. Furthermore, recalling that $x^\top S x = 0$ for any $x \in \mathbb{R}^3$ and any skew-symmetric matrix S, it follows that $\bar{\omega}^\top \Sigma \bar{\omega} = 0$. Finally, since $S(x)x = 0$ for any $x \in \mathbb{R}^3$, we have the property that $\mathcal{R}(q)\epsilon = \epsilon$, for any $q = (\eta, \epsilon) \in \mathcal{S}^3$. It follows that $2\tilde{c}(1 - \tilde{h}\dot{\tilde{\eta}}) = \tilde{c}\tilde{h}\tilde{\epsilon}^\top(\bar{\omega} - u_2)$.

Now, since $\bar{\omega} = \bar{\omega} + \tilde{b} - \tilde{b} = \omega + b - \hat{b} - \bar{\omega}_d + \tilde{b} = \hat{\omega} - \bar{\omega}_d + \tilde{b}$, setting $U_i = \mathcal{K}_i$ yields

$$\left\langle \nabla V_i(\bar{x}_i), \overline{F}_i(\bar{x}_i) \right\rangle = \begin{cases} -\bar{\omega}^\top \Phi(\bar{\omega}) \leq 0 & i = 1 \\ -\tilde{c}\tilde{\epsilon}^\top \tilde{K}\tilde{\epsilon} \leq 0 & i = 2 \\ -\tilde{c}\tilde{\epsilon}^\top \tilde{K}\tilde{\epsilon} - (\hat{\omega} - \bar{\omega}_d)^\top \Phi(\hat{\omega} - \bar{\omega}) - \leq 0 & i = 3 \end{cases} \tag{37}$$

So, we have that $\left\langle \nabla V_i(\bar{x}_i), \overline{F}_i(\bar{x}_i) \right\rangle \leq 0$ for all $\bar{x}_i \in \mathcal{X}_i \supset C_i$.

Now, we examine the change in V_i over jumps. Since $x\overline{\mathrm{sgn}}(x) = |x|$, for every $\bar{x}_i \in D_i$ and every $g \in \overline{G}_i(\bar{x}_i)$,

$$V_i(g) - V_i(\bar{x}_i) = \begin{cases} 2\bar{c}(\bar{h}\bar{\eta} - |\bar{\eta}|) & i = 1 \\ 2\bar{c}(\bar{h}\bar{\eta} - |\bar{\eta}|) + 2\tilde{c}(\tilde{h}\tilde{\eta} - |\tilde{\eta}|) & i = 2, 3. \end{cases} \tag{38}$$

Then, by virtue of $\bar{x}_i \in D_i$, it follows that when $i = 1$, $\bar{h}\bar{\eta} \leq -\delta$ and $-|\bar{\eta}| \leq -\delta$, so $2\bar{c}(\bar{h}\bar{\eta} - |\bar{\eta}|) \leq -4\bar{c}\delta$. For, $i = 2, 3$, we have either that $2\bar{c}(\bar{h}\bar{\eta} - |\bar{\eta}|) \leq -4\bar{c}\delta$ or that $2\tilde{c}(\tilde{h}\tilde{\eta} - |\tilde{\eta}|) \leq -4\tilde{c}\delta$, and the other term can be upper bounded by zero. So, it follows that for all $i \in \{1, 2, 3\}$, $\bar{x}_i \in D_i$ and $g \in \overline{G}_i(\bar{x}_i)$, we have $V_i(g) - V_i(\bar{x}_i) \leq -4\min\{\bar{c}, \tilde{c}\}\delta < 0$.

So far, we have established that the function V_i is monotonically nonincreasing along flows of the closed-loop system and is strictly decreasing along jumps. Applying [44, Theorem 7.6] asserts that $\mathcal{A}_i$ is stable for $\overline{\mathcal{H}}_i$.

To complete the proof, we will apply an invariance principle for hybrid systems. In this direction, let

$$\begin{aligned} W_i &= \{\bar{x}_i \in C_i : \left\langle V_i(\bar{x}_i), \overline{F}_i(\bar{x}_i) \right\rangle = 0\} \Leftrightarrow \\ W_1 &= \{\bar{x}_1 \in \mathcal{X}_1 : \bar{\omega} = 0,\ \bar{h}\bar{\eta} \geq -\delta\} \\ W_2 &= \{\bar{x}_2 \in \mathcal{X}_2 : \tilde{\epsilon} = 0,\ \bar{h}\bar{\eta} \geq -\delta,\ \tilde{h}\tilde{\eta} \geq -\delta\} \\ W_3 &= \{\bar{x}_3 \in \mathcal{X}_3 : \tilde{\epsilon} = \hat{\omega} - \bar{\omega}_d = 0,\ \bar{h}\bar{\eta} \geq -\delta,\ \tilde{h}\tilde{\eta} \geq -\delta\}. \end{aligned} \tag{39}$$

Since V_i is nonincreasing along flows and strictly decreasing over jumps of the i^{th} closed-loop system for every $i \in \{1, 2, 3\}$, applying [44, Theorem 4.7] asserts that $\bar{x}_i$ must converge to the largest invariant set in W_i. We proceed with this argument for $i = 3$, as it is the most involved and note that the cases for $i = 1, 2$ are quite similar.

Constraining $\tilde{\epsilon} \equiv 0$ implies that $\tilde{q} = \pm\mathbf{1}$. Since $\tilde{h}\tilde{\eta} \geq -\delta$, it must follow that $\tilde{q} = h\mathbf{1}$. Continuing, we must have that $\dot{\tilde{q}} \equiv 0$. Then, since $\mathcal{R}(\tilde{q})^\top = \mathcal{R}(h\mathbf{1})^\top = I$, from (34), we see that this can only occur when $\bar{\omega} \equiv 0$ and so, $\dot{\bar{\omega}} = 0$. But, since $\hat{\omega} - \bar{\omega}_d \equiv 0$ and $\hat{\omega} - \bar{\omega}_d = \bar{\omega} - \tilde{b}$, it follows that $\tilde{b} \equiv 0$. Finally, from the evolution of $\bar{\omega}$, it follows that $\bar{\epsilon} \equiv 0$, and since $\bar{h}\bar{\eta} \geq -\delta$, we have $\bar{q} = \bar{h}\mathbf{1}$. This proves that $\mathcal{A}_3$ is globally attractive and hence, globally asymptotically stable. Similarly, it follows that $\mathcal{A}_1$ and $\mathcal{A}_2$ are also globally asymptotically stable for their respective closed-loop systems. ∎

Solutions to hybrid systems $\mathcal{H}$ are parametrized in terms of both t, the amount of time spent flowing, and j, the number of jumps; hence the value of the solution at (t, j) is given by $x(t, j)$. The domain of a solution x is a subset of $\mathbb{R} \times$

[1] A set-valued mapping F is *outer semicontinuous* if its graph, the set $\{(x, y) : y \in F(x)\}$, is closed. Let $\mathbb{B} \subset \mathbb{R}^n$ denote the closed unit ball centered at the origin, then F is *locally bounded* if for any compact set $K \subset \mathbb{R}^n$, there exists $m > 0$ such that $F(K) \subset m\mathbb{B}$.

$\{0,1,2,\dots\}$ and is called a *hybrid time domain* while the function defining the value of the solution is called a *hybrid arc*. We denote the set of solutions starting from a point x_0 or a compact set K as $\mathcal{S}_{\mathcal{H}}(x_0)$ and $\mathcal{S}_{\mathcal{H}}(K)$, respectively. Zeno solutions–those with an infinite number of jumps in a finite amount of time–do not appear in the controllers designed here. In fact, for any solution, the number of jumps is bounded.

Theorem 5.3: For any $i = 1,2,3$, and any compact set $K_i \subset \mathcal{X}_i$, there exists $J_i \in \mathbb{Z}_{\geq 0}$ such that for any $\bar{x}_i \in \mathcal{S}_{\overline{\mathcal{H}}_i}(K_i)$, $\operatorname{dom}\bar{x}_i \subset \mathbb{R}_{\geq 0} \times \{0,1,\dots,J_i\}$.

Proof: Since V_i is continuous and K_i is compact for each $i \in \{1,2,3\}$, let $V_i^* = \max V_i(K_i)$. Then, it follows from (37) and (38) that for any $\bar{x}_i \in \mathcal{S}_{\overline{\mathcal{H}}_i}(\mathcal{X}_i)$ and any $(t,j) \in \operatorname{dom}\bar{x}_i$,

$$0 \leq V_i(\bar{x}_i(t,j)) \leq V_i(\bar{x}_i(0,0)) - 4\delta \min\{\bar{c},\tilde{c}\}j.$$

It follows that for any $\bar{x}_i \in \mathcal{S}_{\overline{\mathcal{H}}_i}(K_i)$ and any $(t,j) \in \operatorname{dom}\bar{x}_i$,

$$j \leq J_i := \left\lceil \tfrac{V_i^*}{4\delta \min\{\bar{c},\tilde{c}\}} \right\rceil,$$

where $\lceil\cdot\rceil$ denotes the ceiling function. ■

Theorem 5.3 gives a uniform bound on the number of jumps occurring along solutions that begin from a given compact set. The number of jumps is linked to initial kinetic energy of the system: as initial bias and angular velocity errors cause the rigid body to rotate, $\bar{q}$ and $\tilde{q}$ can make many revolutions around $\mathcal{S}^3$. During each revolution, it is possible for $\bar{\eta}$ or $\tilde{\eta}$ to initiate jumps. After some of the kinetic energy has been dissipated, the rigid body can no longer rotate past 180° and cause jumps to occur.

We now state a theorem asserting the robustness of the asymptotic stability property asserted in Theorem 5.2 to a general "outer" (see [39]) perturbation that includes both measurement and modeling error. We perturb $\overline{\mathcal{H}}_i$ as follows, resulting in a hybrid inclusion. Let $x_{u,i}$ denote the *unknown* states for each $i = 1,2,3$, i.e., $x_{u,1} = \emptyset$, $x_{u,2} = \omega$, $x_{u,3} = b$. Then, let $T_i : \mathcal{X}_i \to \mathcal{X}_i$ denote the invertible transformation satisfying $T_i(x_i) = \bar{x}_i$ for each $i = 1,2,3$. Now, we define, $\overline{\mathcal{H}}_i^\alpha = (\overline{F}_i^\alpha, \overline{G}_i^\alpha, C_i^\alpha, D_i^\alpha)$, where $\alpha > 0$ and

$$\begin{aligned}
\overline{F}_i^\alpha(\bar{x}_i) &= \overline{\text{co}}F_i(\bar{x}_i, \mathcal{K}_i(y_i + \alpha\mathbb{B}, x_{k,i}, \dot{\omega}_d) + \alpha\mathbb{B}) \\
\overline{G}_i^\alpha(\bar{x}_i) &= \{z \in \mathcal{X}_i : z \in G_i(\bar{x}_i, \mathcal{K}_i(y_i + \alpha\mathbb{B}, x_{k,i}, \dot{\omega}_d))\} \\
C_i^\alpha &= \{\bar{x}_i \in \mathcal{X}_i : T_i(y_i + \alpha\mathbb{B}, x_{u,i}, x_{k,i}) \cap C_i \neq \emptyset\} \\
D_i^\alpha &= \{\bar{x}_i \in \mathcal{X}_i : T_i(y_i + \alpha\mathbb{B}, x_{u,i}, x_{k,i}) \cap D_i \neq \emptyset\}.
\end{aligned} \tag{40}$$

Theorem 5.4: Let V_i be defined as in (35) *and let the conditions of Theorem 5.2 hold. Then, for each $i = 1,2,3$, there exists a class-$\mathcal{KL}$ function β_i such that for each compact set $K_i \subset \mathcal{X}_i$ and every $\gamma_i > 0$, there exists $\alpha_i^* > 0$ such that for all $\alpha \in (0, \alpha_i^*]$, every solution $\bar{x}_i^\alpha \in \mathcal{S}_{\overline{\mathcal{H}}_i^\alpha}(K_i)$ satisfies*

$$V_i(\bar{x}_i^\alpha(t,j)) \leq \beta_i(V_i(\bar{x}_i^\alpha(0,0)), t+j) + \gamma_i \quad \forall (t,j) \in \operatorname{dom}\bar{x}_i^\alpha.$$

Moreover, if $\gamma < 4\delta\min\{\bar{c},\tilde{c}\}$, then there exists $J_i \in \mathbb{Z}_{\geq 0}$ such that $\operatorname{dom}\bar{x}_i^\alpha \subset \mathbb{R}_{\geq} \times \{0,1,\dots,J_i\}$.

Proof: Given Lemma 5.1 and Theorem 5.2, [39, Theorem 6.5] asserts the existence of $\beta_i \in \mathcal{KL}$ such that for all $\bar{x}_i \in \mathcal{S}_{\overline{\mathcal{H}}_i}(\mathcal{X}_i)$,

$$V_i(\bar{x}_i(t,j)) \leq \beta_i(V_i(\bar{x}_i(0,0)), t+j) \qquad \forall (t,j) \in \operatorname{dom}\bar{x}_i.$$

Then, since the family of perturbed systems $\overline{\mathcal{H}}_i^\alpha$ satisfies the convergence property [39, (CP)], we invoke [39, Theorem 6.6] to arrive at the $\mathcal{KL}$ bound on $V_i(\bar{x}_i^\alpha(t,j))$. Then, since $V_i(\bar{x}_i^\alpha(t,j)) \to [0,\gamma] \subset [0, 4\delta\min\{\bar{c},\tilde{c}\})$ as $t+j \to \infty$, we can use similar arguments to Theorem 5.3 to arrive at a bound on the number of jumps. ■

Note that we can always choose K to include the entirety of $\mathcal{S}^3$ for the states q_d, $\bar{q}$, and $\tilde{q}$; hence, the $\mathcal{KL}$ estimate holds for any initial orientation of the rigid body. On the other hand, K cannot be chosen to include all initial angular velocities, since they evolve in $\mathbb{R}^3$ which is not compact.

E. Measurement Noise and Chattering

When the hybrid controller is subjected to measurement noise, it is possible for chattering to occur, which manifests in the closed-loop hybrid system as the possibility of multiple jumps occurring at the same time. This is possible when jumps can map the state back into the jump set, that is, when $G(D) \cap D \neq \emptyset$. To eliminate the possibility of chattering for a bounded noise signal, we compute a lower bound on the distance between $\overline{G}_i^\alpha(D_i^\alpha)$ and D_i^α, defined in (40). We provide these bounds for $i = 1,2,3$, but only provide the proof for $i = 2,3$, as the case for $i = 1$ is similar and simpler. We state these bounds in the following theorem.

Theorem 5.5: For every $\alpha \in [0, \frac{1}{2})$ and every $\delta \in (2\alpha, 1)$, $D_i^\alpha \cap \overline{G}_i^\alpha(D_i^\alpha) = \emptyset$.

Proof: ($i = 2,3$) First, we note a helpful characterization of $\overline{G}_i^\alpha(D_i^\alpha)$. Using properties of quaternions, a calculation shows that

$$D_i^\alpha = \{\bar{x}_i \in \mathcal{X}_i : \bar{h}\bar{\eta} \leq -\delta + \alpha \text{ or } \tilde{h}\tilde{\eta} \leq -\delta + \alpha\}.$$

Since states other than $\bar{h}$, $\tilde{h}$, $\bar{q}$ and $\tilde{q}$ do not enter into the constraints defining D_i^α and since $\bar{q}$ and $\tilde{q}$ do not change over jumps, we only examine the jump equations for $\bar{h}$ and $\tilde{h}$ when perturbed by measurement noise. As before, we can employ basic properties of quaternions to arrive at

$$\bar{h}^+ \in \overline{\text{sgn}}(\bar{\eta} + \alpha\mathbb{B}) \qquad \tilde{h}^+ \in \overline{\text{sgn}}(\tilde{\eta} + \alpha\mathbb{B}). \tag{41}$$

It is helpful to note that (41) is equivalent to writing $\bar{h}^+\bar{\eta} \geq -\alpha$ and $\tilde{h}^+\tilde{\eta} \geq -\alpha$.

With this observation, we can write $\overline{G}_i^\alpha(D_i^\alpha)$ as

$$\begin{aligned}
\overline{G}_i^\alpha(D_i^\alpha) = &\{\bar{x}_i \in \mathcal{X}_i : \bar{h}\bar{\eta} \geq -\alpha \text{ and } \tilde{h}\tilde{\eta} \geq -\alpha\} \\
&\cap \{\bar{x}_i \in \mathcal{X}_i : |\bar{\eta}| \geq \delta - \alpha \text{ or } |\tilde{\eta}| \geq \delta - \alpha\}.
\end{aligned}$$

In preparation for computing $\text{dist}(D_i^\alpha, \overline{G}_i^\alpha(D_i^\alpha))$, we decompose D_i^α and $\overline{G}_i^\alpha(D_i^\alpha)$ into the unions

$$D_i^\alpha = \Delta_{i,1}^\alpha \cup \Delta_{i,2}^\alpha \quad \overline{G}_i^\alpha(D_i^\alpha) = \Gamma_{i,1}^\alpha \cup \Gamma_{i,2}^\alpha,$$

where

$$\begin{aligned}
\Delta_{i,1}^\alpha &= \{\bar{x}_i \in \mathcal{X}_i : \bar{h}\bar{\eta} \leq -\delta + \alpha\} \\
\Delta_{i,2}^\alpha &= \{\bar{x}_i \in \mathcal{X}_i : \tilde{h}\tilde{\eta} \leq -\delta + \alpha\} \\
\Gamma_{i,1}^\alpha &= \{\bar{x}_i \in \mathcal{X}_i : \bar{h}\bar{\eta} \geq -\alpha \text{ and } \tilde{h}\tilde{\eta} \geq -\alpha\} \\
&\quad \cap \{\bar{x}_i \in \mathcal{X}_i : |\bar{\eta}| \geq \delta - \alpha\} \\
\Gamma_{i,2}^\alpha &= \{\bar{x}_i \in \mathcal{X}_i : \bar{h}\bar{\eta} \geq -\alpha \text{ and } \tilde{h}\tilde{\eta} \geq -\alpha\} \\
&\quad \cap \{\bar{x}_i \in \mathcal{X}_i : |\tilde{\eta}| \geq \delta - \alpha\}.
\end{aligned}$$

Intending to break the distance computation into simpler pieces, we note that

$$\text{dist}(D_i^\alpha, \overline{G}_i^\alpha(D_i^\alpha)) = \min_{j,k\in\{1,2\}} \text{dist}(\Delta_{i,j}^\alpha, \Gamma_{i,k}^\alpha).$$

Let

$$\Gamma_i^\alpha = \{\bar{x}_i \in \mathcal{X}_i : \bar{h}\bar{\eta} \geq -\alpha \text{ and } \tilde{h}\tilde{\eta} \geq -\alpha\}.$$

Then, it follows that $\overline{G}_i^\alpha(D_i^\alpha) \subset \Gamma_i^\alpha$ and

$$\text{dist}(D_i^\alpha, \overline{G}_i^\alpha(D_i^\alpha)) \geq \text{dist}(D_i^\alpha, \Gamma_i^\alpha) = \min_{j\in\{1,2\}} \text{dist}(\Delta_{i,j}^\alpha, \Gamma_i^\alpha).$$

Using the norm $|h_1 - h_2|$ for elements $h_1, h_2 \in H$ and $\|q_1 - q_2\|_2$ for $q_1, q_2 \in \mathcal{S}^3$, it follows that for $q_1 = (\eta_1, \epsilon_1)$ and $q_2 = (\eta_2, \epsilon_2)$, $\|q_1 - q_2\|_2 \geq |\eta_1 - \eta_2|$. Then, it follows that

$$\begin{aligned}
\text{dist}(\Delta_{i,1}^\alpha, \Gamma_i^\alpha) &\geq \min_{\substack{h,k\in\{-1,1\}\\ -1\leq\bar{h}\bar{\eta}\leq-\delta+\alpha\\ -\alpha\leq\bar{k}\bar{\xi}\leq 1}} |\bar{h} - \bar{k}| + |\bar{\eta} - \bar{\xi}| \\
\text{dist}(\Delta_{i,2}^\alpha, \Gamma_i^\alpha) &\geq \min_{\substack{\tilde{h},\tilde{k}\in\{-1,1\}\\ -1\leq\tilde{h}\tilde{\eta}\leq-\delta+\alpha\\ -\alpha\leq\tilde{k}\tilde{\xi}\leq 1}} |\tilde{h} - \tilde{k}| + |\tilde{\eta} - \tilde{\xi}|
\end{aligned} \tag{42}$$

Note that the right-hand sides of the expressions in (42) are identical. In this direction, we examine only one of them. Since $\bar{h}, \bar{k} \in \{-1, 1\}$, we break the minimization into four cases. First, suppose that $\bar{h} = \bar{k}$. It follows that $-2 \leq \bar{h}(\bar{\eta} - \bar{\xi}) \leq -\delta + 2\alpha$. Now suppose that $\bar{h} \in \overline{\text{sgn}}(\bar{\eta} - \bar{\xi})$ so that $-2 \leq |\bar{\eta} - \bar{\xi}| \leq -\delta + 2\alpha$, in which case,

$$\min_{-2\leq|\bar{\eta}-\bar{\xi}|\leq-\delta+2\alpha} |\bar{h} - \bar{k}| + |\bar{\eta} - \bar{\xi}| = \begin{cases} \emptyset & \delta > 2\alpha \\ 0 & \delta \leq 2\alpha. \end{cases}$$

Now supposing that $\bar{h} \in -\overline{\text{sgn}}(\bar{\eta} - \bar{\xi})$, it follows that $2\alpha - \delta \leq |\bar{\eta} - \bar{\xi}| \leq 2$ and

$$\min_{2\alpha-\delta\leq|\bar{\eta}-\bar{\xi}|\leq 2} |\bar{h} - \bar{k} + |\bar{\eta} - \bar{\xi}| = \max(0, 2\alpha - \delta).$$

We handle the other two cases in a similar fashion. Let $\bar{h} = -\bar{k}$ and suppose that $\bar{h} \in \overline{\text{sgn}}(\bar{\eta} - \bar{\xi})$, then $-1 - \alpha \leq |\bar{\eta} - \bar{\xi}| \leq 1 + \alpha - \delta$ and

$$\min_{-1-\alpha\leq|\bar{\eta}-\bar{\xi}|\leq 1+\alpha-\delta} |\bar{h} - \bar{k}| + |\bar{\eta} - \bar{\xi}| = 2.$$

Similarly, when $\bar{h} \in -\overline{\text{sgn}}(\bar{\eta} - \bar{\xi})$, it follows that $\delta - 1 - \alpha \leq |\bar{\eta} - \bar{\xi}| \leq 1 + \alpha$ and

$$\min_{\delta-1-\alpha\leq|\bar{\eta}-\bar{\xi}|\leq 1+\alpha} |\bar{h} - \bar{k}| + |\bar{\eta} - \bar{\xi}| = 2.$$

Finally, since

$$\begin{aligned}
\text{dist}(D_i^\alpha, \overline{G}_i^\alpha(D_i^\alpha)) &\geq \min_{j\in\{1,2\}} \text{dist}(\Delta_{i,j}^\alpha, \Gamma_i^\alpha) \\
&\geq \min(\max(0, 2\alpha - \delta), 2) \\
&= \max(0, 2\alpha - \delta),
\end{aligned}$$

selecting $\delta > 2\alpha$ yields $\text{dist}(D_i^\alpha, \overline{G}_i^\alpha(D_i^\alpha)) > 0$ and $D_i^\alpha \cap \overline{G}_i^\alpha(D_i^\alpha) = \emptyset$. ■

VI. Simulation Study

In this section, we present a simulation study contrasting the proposed hybrid control scheme with both a discontinuous controller and a controller that induces unwinding. We contrast these controllers in two scenarios that illustrate how unwinding can cause undesirable behavior and how the discontinuous controller is sensitive to measurement noise. The following simulations correspond to the full-state-measurement case, where both q and ω are measured without any additive bias on ω, as in Section V-A. In each case, the rigid body is commanded to come to rest at a specified attitude. In particular, we let $q_d(0) = \mathbf{1}$, $\omega_d(0) = 0$, and $\dot{\omega}_d \equiv 0$ (note that $\bar{q} = q$ here). Further, let $\vec{v} = [1\ 2\ 3]^\top$, $v = \vec{v}/\|\vec{v}\|_2$. Then, the inertia matrix and control parameters are given as $\mathcal{J} = \text{diag}(10v)$, $\bar{c} = 1$ and $\Phi(\omega) = \omega$. The simulations were conducted in MATLAB/Simulink using a variable-step solver (ode45) constrained to a maximum step size of $1/1000$s. While the norm of quaternion states may drift from 1 in a numerical implementation, the effects of numerical drift were negligible in the following simulations. Regardless, all quaternion variables corresponding to an attitude were projected to $\mathcal{S}^3$ before used in any manner.

Each plot in the following simulations is labeled as either *hybrid*, *discontinuous*, or *unwinding*. For each plot labeled hybrid, the hysteresis half-width is chosen as $\delta = 0.4$. When the hysteresis width becomes zero ($\delta = 0$), the control reduces to the discontinuous scheme, essentially replacing $\bar{h}$ with $\text{sgn}(\bar{\eta})$. When $\delta > 1$, jumps are completely disabled, since $|\eta| \leq 1$. In this case, $\bar{h}$ is a constant corresponding to its initial condition. In each of the following simulations, $\bar{h}(0) = 1$, which, when $\delta > 1$, has the effect of stabilizing $\bar{q} = +\mathbf{1}$ only. In this direction, plots labeled as discontinuous have $\delta = 0$ and plots labeled as unwinding have $\delta > 1$.

Finally, each figure has 4 plots: $\bar{h}\bar{\eta}$, $\theta(\bar{q})$, $\|\bar{\omega}\|_2$, and $\sqrt{\int_0^t \tau^\top \tau dt}$. The plot of $\bar{h}\bar{\eta}$ is shown to illustrate its convergence towards 1 and jumps in $\bar{h}$. In the unwinding case, because $\bar{h} \equiv \bar{h}(0) = 1$, this corresponds to a plot of $\bar{\eta}$. The plot of $\theta(\bar{q}) = 2\cos^{-1}|\bar{\eta}|$ is the angle between the current attitude and the desired attitude. The plots of $\|\bar{\omega}\|_2$ and $\sqrt{\int_0^t \tau^\top \tau dt}$ show convergence of angular rate error and the use of control effort, respectively.

Fig. 3 illustrates noise sensitivity when $\delta = 0$ (i.e. for discontinuous feedback including terms like $\text{sgn}(\bar{\eta})\bar{\epsilon}$). In this simulation, $q(0) = (0, v)$ and $\omega(0) = 0$. The measured value of q is $q_m = (q + me)/\|q + me\|_2$, where $e = \vec{e}/\|\vec{e}\|_2$, each element of $\vec{e}$ was drawn from a zero-mean Gaussian distribution with unit variance, and m was drawn from a uniform distribution on the interval $[0, 0.2]$. This causes a chattering behavior, visible in the plot of $\bar{h}\bar{\eta}$ for the discontinuous control law. In this case, the excessive chattering causes a lag in response and unnecessarily wasted control effort. On the other hand, the hybrid controller is largely impervious to the noise (concerning the decision of which way to rotate), owning to the sufficiently large selection of δ. In this simulation, the unwinding controller is not shown, as the resulting trajectory is identical to the hybrid controller (this is because $\bar{h}$ doesn't change in this simulation and $\bar{h}(0) = 1$).

Preprint submitted to IEEE Transactions on Automatic Control. Received: January 18, 2011 20:37:59 PST

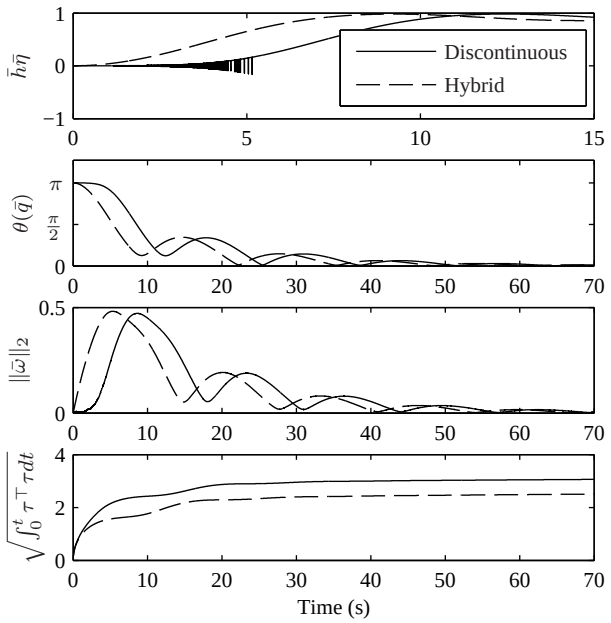

Fig. 3. Noise sensitivity.

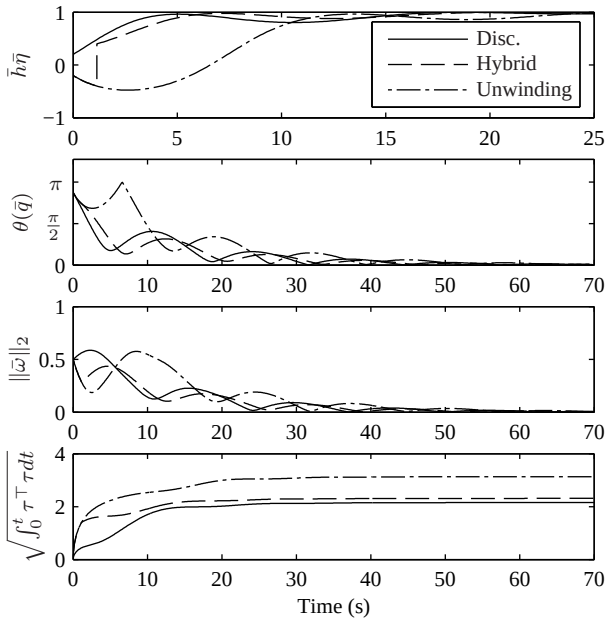

Fig. 4. Effects of unwinding.

Fig. 4 shows how control laws that exhibit unwinding can resist a "beneficial" initial angular velocity. In this simulation, $q(0) = (-0.2, \sqrt{1-0.2^2}v)$ and $\omega(0) = 0.5v$. So, the initial angular velocity is in a direction that *decreases* the angle between the initial rigid body attitude and the desired attitude, i.e., η (and also $\bar{\eta}$ in this case) will initially decrease from -0.2 towards -1. In this simulation, the discontinuous control law immediately pulls the attitude towards $\bar{q} = -\mathbf{1}$. Due to the hysteresis and the fact that $\bar{h} = 1$, the hybrid control law initially pulls the attitude towards $q = +\mathbf{1}$, but after the initial angular velocity pushes the attitude past the hysteresis width (at approximately 2s), its value of $\bar{h}$ switches and then pulls the attitude towards $q = -\mathbf{1}$. On the other hand, the unwinding-inducing control law *always* pulls the attitude towards $\bar{q} = +\mathbf{1}$ and in this simulation, expends more control effort doing so.

VII. Conclusion

We reviewed the topological problems associated with global attitude control and illustrated how quaternion-based discontinuous control laws that are intended to solve the global asymptotic stabilization problem are susceptible to measurement noise. In fact, we illustrated how malicious measurement noise can enter into the closed-loop system and have an asymptotically stabilizing effect on the manifold of 180° rotations.

We proposed a hybrid control solution to these problems that achieves robust global asymptotic tracking for several measurement scenarios. Drawing on previous work, the hybrid control scheme employs a logic variable that defines the desired direction of rotation. By using a hysteretic switching law, the hybrid scheme can mitigate the unwanted effects of unwinding and chattering due to measurement noise. Moreover, the hybrid scheme allows the control designer to choose the hysteresis width, which effectively manages a trade-off between robustness to measurement noise and hysteresis-induced inefficiency.

These results were supported by simulation, where the proposed hysteretic controller was compared to a discontinuous controller and a controller that induces unwinding. As desired, the proposed hybrid controller was seen to avoid unwinding and eliminated extreme measurement noise sensitivity present in discontinuous feedbacks that can delay control response and waste energy.

References

[1] V. Guillemin and A. Pollack, *Differential Topology*. Prentice-Hall, Inc., 1974.
[2] E. Sontag, *Mathematical Control Theory*. Springer, 1998.
[3] N. P. Bhatia and G. P. Szegö, *Stability Theory of Dynamical Systems*. Springer, 1970.
[4] S. P. Bhat and D. S. Bernstein, "A topological obstruction to continuous global stabilization of rotational motion and the unwinding phenomenon," *Systems & Control Letters*, vol. 39, no. 1, pp. 63–70, Jan. 2000.
[5] D. E. Koditschek, "The application of total energy as a Lyapunov function for mechanical control systems," in *Dynamics and Control of Multibody Systems*, ser. Contemporary Mathematics, J. E. Marsden, P. S. Krishnaprasad, and J. C. Simo, Eds. American Mathematical Society, 1989, vol. 97, pp. 131–157.
[6] N. A. Chaturvedi and N. H. McClamroch, "Almost global attitude stabilization of an orbiting satellite including gravity gradient and control saturation effects," in *Proceedings of the 2006 American Control Conference*, 2006, pp. 1748–1753.
[7] A. Sanyal, A. Fosbury, N. A. Chaturvedi, and D. S. Bernstein, "Inertia-free spacecraft attitude tracking with disturbance rejection and almost global stabilization," *Journal of Guidance, Control, and Dynamics*, vol. 32, no. 4, pp. 1167–1178, 2009.
[8] N. A. Chaturvedi, N. H. McClamroch, and D. S. Bernstein, "Asymptotic smooth stabilization of the inverted 3-D pendulum," *IEEE Transactions on Automatic Control*, vol. 54, no. 6, pp. 1204–1215, 2009.
[9] S. Bertrand, T. Hamel, H. Piet-Lahanier, and R. Mahony, "Attitude tracking of rigid bodies on the special orthogonal group with bounded partial state feedback," in *Proceedings of the 48th IEEE Conference on Decision and Control*, 2009.
[10] N. Chaturvedi and H. McClamroch, "Asymptotic stabilization of the inverted equilibrium manifold of the 3-D pendulum using non-smooth feedback," *IEEE Transactions on Automatic Control*, vol. 54, no. 11, pp. 2658–2662, Nov. 2009.

[11] N. Chaturvedi, T. Lee, M. Leok, and N. McClamroch, "Nonlinear dynamics of the 3D pendulum," *Journal of Nonlinear Science*, pp. 1–30, 2010.
[12] J. Yuan, "Closed-loop manipulator control using quaternion feedback," *IEEE Journal of Robotics and Automation*, vol. 4, no. 4, pp. 434–440, Aug. 1988.
[13] J. Osborne, G. Hicks, and R. Fuentes, "Global analysis of the double-gimbal mechanism," *IEEE Control Systems Magazine*, vol. 28, no. 4, pp. 44–64, 2008.
[14] J. Stuelpnagel, "On the parametrization of the three-dimensional rotation group," *SIAM Review*, vol. 6, no. 4, pp. 422–430, Oct. 1964.
[15] B. Wie and P. M. Barba, "Quaternion feedback for spacecraft large angle maneuvers," *Journal of Guidance, Control, and Dynamics*, vol. 8, no. 3, pp. 360–365, 1985.
[16] J. T.-Y. Wen and K. Kreutz-Delgado, "The attitude control problem," *IEEE Transactions on Automatic Control*, vol. 36, no. 10, pp. 1148–1162, Oct. 1991.
[17] O. Egeland and J.-M. Godhavn, "Passivity-based adaptive attitude control of a rigid spacecraft," *IEEE Transactions on Automatic Control*, vol. 39, no. 4, pp. 842–846, Apr. 1994.
[18] S. M. Joshi, A. G. Kelkar, and J. T.-Y. Wen, "Robust attitude stabilization of spacecraft using nonlinear quaternion feedback," *IEEE Transactions on Automatic Control*, vol. 40, no. 10, pp. 1800–1803, 1995.
[19] F. Lizarralde and J. T. Wen, "Attitude control without angular velocity measurement: a passivity approach," *IEEE Transactions on Automatic Control*, vol. 41, no. 3, pp. 468–472, Mar. 1996.
[20] A. Tayebi, "Unit quaternion-based output feedback for the attitude tracking problem," *IEEE Transactions on Automatic Control*, vol. 53, no. 6, pp. 1516–1520, Jul. 2008.
[21] R. G. Sanfelice, M. J. Messina, S. E. Tuna, and A. R. Teel, "Robust hybrid controllers for continuous-time systems with applications to obstacle avoidance and regulation to disconnected set of points," in *Proceedings of the American Control Conference*, 2006, pp. 3352–3357.
[22] S. Salcudean, "A globally convergent angular velocity observer for rigid body motion," *IEEE Transactions on Automatic Control*, vol. 36, no. 12, pp. 1493–1497, Dec. 1991.
[23] J. Thienel and R. M. Sanner, "A coupled nonlinear spacecraft attitude controller and observer with an unknown constant gyro bias and gyro noise," *IEEE Transactions on Automatic Control*, vol. 48, no. 11, pp. 2011–2015, Nov. 2003.
[24] D. Fragopoulos and M. Innocenti, "Stability considerations in quaternion attitude control using discontinuous Lyapunov functions," *IEE Proceedings - Control Theory and Applications*, vol. 151, no. 3, pp. 253–258, May 2004.
[25] R. Kristiansen, P. J. Nicklasson, and J. T. Gravdahl, "Satellite attitude control by quaternion-based backstepping," *IEEE Transactions on Control Systems Technology*, vol. 17, no. 1, pp. 227–232, Jan. 2009.
[26] C. Prieur, R. Goebel, and A. Teel, "Hybrid feedback control and robust stabilization of nonlinear systems," *IEEE Transactions on Automatic Control*, vol. 52, no. 11, pp. 2103–2117, Nov. 2007.
[27] Z. Artstein, "Stabilization with relaxed controls," *Nonlinear Analysis*, vol. 7, no. 11, pp. 1163–1173, 1983.
[28] E. Sontag, "Clocks and insensitivity to small measurement errors," *Control, Optimisation and Calculus of Variations*, vol. 4, pp. 537–557, Oct. 1999.
[29] J. R. Munkres, *Topology*. Prentice Hall, 2000.
[30] M. D. Shuster, "A survey of attitude representations," *The Journal of the Astronomical Sciences*, vol. 41, no. 4, pp. 439–517, 1993.
[31] J. K. Kuipers, *Quaternions and Rotation Sequences*. Princeton University Press, 1999.
[32] C. G. Mayhew, R. G. Sanfelice, and A. R. Teel, "Robust global asymptotic attitude stabilization of a rigid body by quaternion-based hybrid feedback," in *Proceedings of the 48th IEEE Conference on Decision and Control and 28th Chinese Control Conference*, 2009, pp. 2522–2527.
[33] B. Wie, H. Weiss, and A. Arapostathis, "Quaternion feedback regulator for spacecraft eigenaxis rotations," *Journal of Guidance, Control, and Dynamics*, vol. 12, no. 3, pp. 375–380, 1989.
[34] O. E. Fjellstad and T. I. Fossen, "Quaternion feedback regulation of underwater vehicles," in *Proceedings of the 3rd IEEE Conference on Control Applications*, vol. 2, 1994, pp. 857–862.
[35] O. Hájek, "Discontinuous differential equations, I," *Journal of Differential Equations*, vol. 32, no. 2, pp. 149–170, May 1979.
[36] H. Hermes, "Discontinuous vector fields and feedback control," in *Differential Equations and Dynamic Systems*, J. K. Hale and J. P. LaSalle, Eds. Academic Press Inc., 1967, pp. 155–165.
[37] N. N. Krasovskii and A. I. Subbotin, *Game-Theoretical Control Problems*. Springer-Verlag, 1988.
[38] J. Aubin and A. Cellina, *Differential Inclusions: Set-Valued Maps and Viability Theory*. Springer-Verlag, 1984.
[39] R. Goebel and A. Teel, "Solutions to hybrid inclusions via set and graphical convergence with stability theory applications," *Automatica*, vol. 42, no. 4, pp. 573–587, Apr. 2006.
[40] P. Pisu and A. Serrani, "Attitude tracking with adaptive rejection of rate gyro disturbances," *IEEE Transactions on Automatic Control*, vol. 52, no. 12, pp. 2374–2379, Dec. 2007.
[41] B. T. Costic, D. M. Dawson, M. S. De Queiroz, and V. Kapila, "A quaternion-based adaptive attitude tracking controller without velocity measurements," in *Proceedings of the 39th IEEE Conference on Decision and Control*, vol. 3, 2000, pp. 2424–2429.
[42] P. Tsiotras, "Further passivity results for the attitude control problem," *IEEE Transactions on Automatic Control*, vol. 43, no. 11, pp. 1597–1600, Nov. 1998.
[43] R. Goebel, R. G. Sanfelice, and A. R. Teel, "Hybrid dynamical systems," *IEEE Control Systems Magazine*, vol. 29, no. 2, pp. 28–93, Apr. 2009.
[44] R. G. Sanfelice, R. Goebel, and A. R. Teel, "Invariance principles for hybrid systems with connections to detectability and asymptotic stability," *IEEE Transactions on Automatic Control*, vol. 52, no. 12, pp. 2282–2297, Dec. 2007.

Christopher G. Mayhew received the B.S. degree in Electrical Engineering from the University of California, Riverside in 2005 and received the M.S. and Ph.D. degrees in Electrical and Computer Engineering from the University of California, Santa Barbara in 2008 and 2010, respectively. He is currently a researcher at the Robert Bosch Research and Technology Center. His research interests include topological constraints in control systems, modeling, control, and simulation of hybrid and nonlinear systems, and battery management systems for automotive applications. He is also a member of Tau Beta Pi.

Ricardo G. Sanfelice received the B.S. degree in electronics engineering from the Universidad de Mar del Plata, Buenos Aires, Argentina, in 2001. He joined the Center for Control, Dynamical Systems, and Computation at the University of California, Santa Barbara in 2002, where he received the M.S. and Ph.D. degrees in 2004 and 2007, respectively. In 2007 and 2008, he held postdoctoral positions at the Laboratory for Information and Decision Systems at the Massachusetts Institute of Technology and at the Centre Automatique et Systmes at the cole de Mines de Paris. In 2009, he joined the faculty of the Department of Aerospace and Mechanical Engineering at the University of Arizona, where he is currently an assistant professor. His research interests are in modeling, stability, robust control, and simulation of nonlinear, hybrid, and embedded systems with applications to robotics, aerospace, and biology.

Andrew R. Teel received his A.B. degree in Engineering Sciences from Dartmouth College in Hanover, New Hampshire, in 1987, and his M.S. and Ph.D. degrees in Electrical Engineering from the University of California, Berkeley, in 1989 and 1992, respectively. After receiving his Ph.D., Dr. Teel was a postdoctoral fellow at the Ecole des Mines de Paris in Fontainebleau, France. In 1992 he joined the faculty of the Electrical Engineering Department at the University of Minnesota where he was an assistant professor. In 1997, Dr. Teel joined the faculty of the Electrical and Computer Engineering Department at the University of California, Santa Barbara, where he is currently a professor.